AD_____

Award Number: W81XWH-11-1-0208

TITLE:
Inhibition of breast cancer progression by blocking heterocellular contact between epithelial cells and fibroblasts

PRINCIPAL INVESTIGATOR:
Professor David J. Beebe

CONTRACTING ORGANIZATION: The University of Wisconsin-Madison
Madison WI 53715-1218

REPORT DATE:
April 2013

TYPE OF REPORT:
Addendum to Final

PREPARED FOR: U.S. Army Medical Research and Materiel Command
Fort Detrick, Maryland 21702-5012

REPORT DOCUMENTATION PAGE

Form Approved
OMB No. 0704-0188

1. REPORT DATE	2. REPORT TYPE	3. DATES COVERED
April 2013	Addendum to Final	1 April 2012 – 31 March 2013

4. TITLE AND SUBTITLE
Inhibition of breast cancer progression by blocking heterocellular contact between epithelial cells and fibroblasts

5a. CONTRACT NUMBER

5b. GRANT NUMBER
W81XWH-11-1-0208

5c. PROGRAM ELEMENT NUMBER

6. AUTHOR(S)
David J. Beebe, Kyung Eun Sung

E-Mail: djbeebe@wisc.edu; kesung@wisc.edu

5d. PROJECT NUMBER

5e. TASK NUMBER

5f. WORK UNIT NUMBER

7. PERFORMING ORGANIZATION NAME(S) AND ADDRESS(ES)
The University of Wisconsin - Madison

Madison WI 53715-1218

8. PERFORMING ORGANIZATION REPORT NUMBER

9. SPONSORING / MONITORING AGENCY NAME(S) AND ADDRESS(ES)
U.S. Army Medical Research and Materiel Command
Fort Detrick, Maryland 21702-5012

10. SPONSOR/MONITOR'S ACRONYM(S)

11. SPONSOR/MONITOR'S REPORT NUMBER(S)

12. DISTRIBUTION / AVAILABILITY STATEMENT
Approved for Public Release; Distribution Unlimited

13. SUPPLEMENTARY NOTES

14. ABSTRACT
In breast cancer progression, the transition from ductal carcinoma in situ (DCIS) to invasive ductal carcinoma (IDC) is a life-threatening step. This step is accompanied by a dramatic drop in prognosis. Stromal fibroblasts and epithelial cells are separated by a basement membrane (BM) at the early DCIS stage. However, once the BM is disrupted and stromal invasion of epithelial cells is initiated, direct heterocellular contacts between fibroblasts and epithelial cells often occurs. This suggests that the signaling through the heterocellular contact may be a crucial factor in how the invasive progress continues after it is initiated. Accordingly, the objective of this proposal is to investigate the influence of heterocellular contacts between MCF-DCIS cells and human mammary fibroblasts (HMFs) in breast cancer progression by employing a microfluidic-based compartmentalized 3D co-culture platform enabling both contact-free and contact-associated co-cultures.

15. SUBJECT TERMS
Heterocellular contact between cancer cells and stromal fibroblasts, Microfluidics, 3D

16. SECURITY CLASSIFICATION OF:			17. LIMITATION OF ABSTRACT	18. NUMBER OF PAGES	19a. NAME OF RESPONSIBLE PERSON
a. REPORT	b. ABSTRACT	c. THIS PAGE			USAMRMC
U	U	U	UU		19b. TELEPHONE NUMBER *(include area code)*

Table of Contents

Introduction

In breast cancer progression, the transition from ductal carcinoma in situ (DCIS) to invasive ductal carcinoma (IDC) is a life-threatening step. This step is accompanied by a dramatic drop in prognosis. Stromal fibroblasts and epithelial cells are separated by a basement membrane (BM) at the early DCIS stage. However, once the BM is disrupted and stromal invasion of epithelial cells is initiated, direct heterocellular contacts between fibroblasts and epithelial cells often occurs. This suggests that the signaling through the heterocellular contact may be a crucial factor in how the invasive progress continues after it is initiated. Accordingly, the objective of this proposal is to investigate the influence of heterocellular contacts between MCF-DCIS cells and human mammary fibroblasts (HMFs) in breast cancer progression by employing a microfluidic-based compartmentalized 3D co-culture platform enabling both contact-free and contact-associated co-cultures. Here we report progress on the project. We have successfully accomplished Specific Aim 1 (these results were reported in the YR1 progress report). In the original proposal under Specific Aim 2, we proposed to try gap junction inhibitors to inhibit the heterocellular contacts between MCF-DCIS cells and HMFs. We did test gap junction inhibitors, but these drugs did not efficiently block the contacts. Thus, in addition we looked at the properties of HMFs near MCF-DCIS cells, and inhibited DCIS progression by blocking the activation of HMFs near MCF-DCIS cells.

Body

In our YR1 progress report, we reported our accomplishments on Aim 1. To summarize, we developed a microscale 3D co-culture platform (Task 1), and validated the existence of heterocellular contacts formed between MCF-DCIS cells and HMF cells in contact-associated co-cultures (Task 2). In addition, we analyzed soluble molecules secreted by HMFs cultured in 2D and 3D conditions and found that the HMFs in a 3D condition secreted higher concentration of a few molecules such as HGF, CXCL12, and MMP14. The HMFs in a 3D condition have higher impact on DCIS progression to IDC. Moreover, by using the microscale compartmentalized 3D co-culture platform, we verified that the HMFs near the MCF-DCIS cells were activated showing a few protrusions. The actin-rich protrusions in HMFs were correlated with local concentration increase of beta-1 integrins suggesting that the protrusions express sticky ends that stimulate adhesion of HMFs to surrounding extracellular matrices as well as to other cells. Using the no cost extension, we explored mechanisms involved in the activation of fibroblasts in co-cultures with MCF-DCIS cells.

1) Investigation of ECM alteration caused by the activation of fibroblasts in proximity to MCF-DCIS cells:

One of the most striking features of HMF cells that have been exposed to the MCF-DCIS secretome is the protrusive, stelate morphology (Fig. 1). These exposed HMF cells also differ from control cells in the way that they alter the surrounding collagen matrix. During YR1, we verified that the signaling based on Cathepsin D (CTSD) produced from MCF-DCIS and low-density lipoprotein receptor-related protein-1 (LRP1) in HMFs was responsible for the protrusive activity of HMFs.

In YR 2, we focused on exploring the alterations in the surrounding ECM caused by the fibroblast activation. Stromal fibroblasts are also major regulators for the alteration of extra cellular matrix (ECM) architecture, which provides particular prognostic information of cancerous tissues. However, the mechanism triggering fibroblasts to cease their normal function and to alter ECM architectures prone to invasion of cancer cells still needs to be understood. We were interested in quantifying some of these qualitative observations in order to more thoroughly study this phenomenon, to identify analytical endpoints that could be used in future screening applications. We did this by examining the cell morphology and the alteration of the surrounding matrix. Quantification of changes to the collagen matrix surrounding the cells was performed concurrently with the morphology quantification by using the TraceMeasure program that we developed through collaboration. Analysis was performed on SHG images corresponding to the images of GPF expressing HMFs used in the morphology quantification. Average SHG intensity and average collagen fiber alignment corresponding to each outline pixel were calculated within a 15 μm region around the border of each HMF.

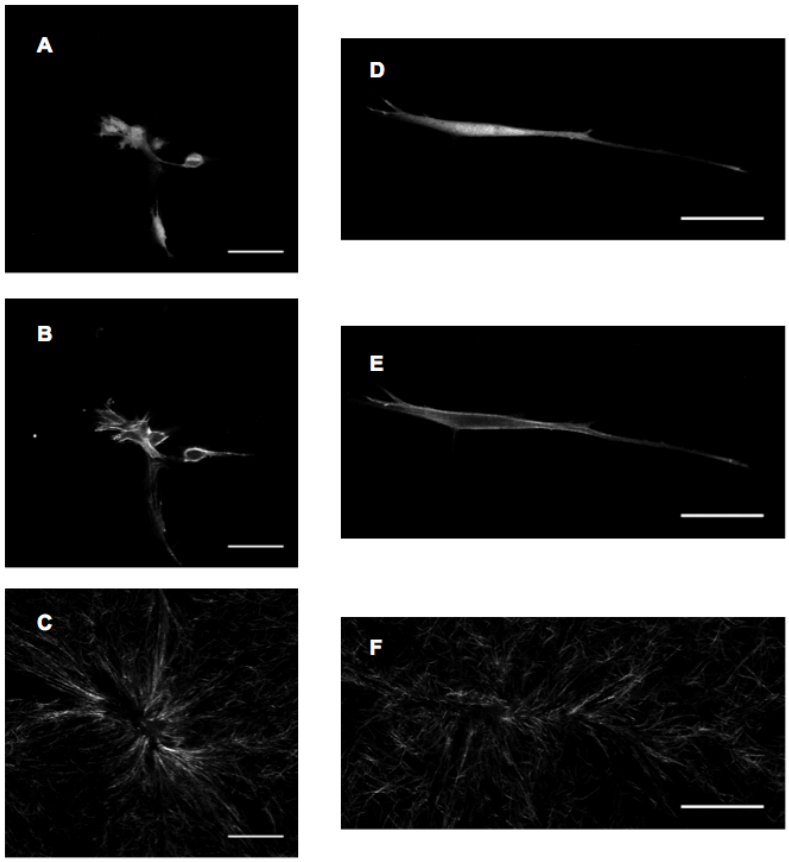

Fig. 1. (A) GFP-expressing HMF cells after exposure to MCF-DCIS secretome. **(B)** Phalloidin staining of cells in (A) showing F-actin structure. **(C)** SHG image showing collagen fibers surrounding cells in (A). **(D)** GFP-expressing HMF in control conditions. **(E)** Phalloidin staining of cell in (D). **(F)** SHG image showing collagen fibers surrounding (D). Scale bars represent 50 μm.

In addition, we identified the relationship between cell protrusions (corresponding to large values in the morphology measurement), areas of high SHG intensity, indicating increased local density of collagen I, and regions in which collagen fibers were oriented perpendicularly to the cell boundary. This was done by finding the Spearman Rank Correlation Coefficient between the derivatives of the data. We found that the correlation between cellular protrusions and SHG intensity as well as cellular protrusions and perpendicularly aligned collagen fibers, was higher for co-cultured fibroblasts than for control (Fig. 2). This supports our findings that HMFs exposed to the DCIS secretome have higher levels of activated beta1 integrin and cell adhesion complexes, enabling them to more extensively remodel the surrounding collagen matrix, thereby creating a denser and more aligned environment for the neighboring DCIS cells, which contributes to the invasive transition seen in these co-cultures.

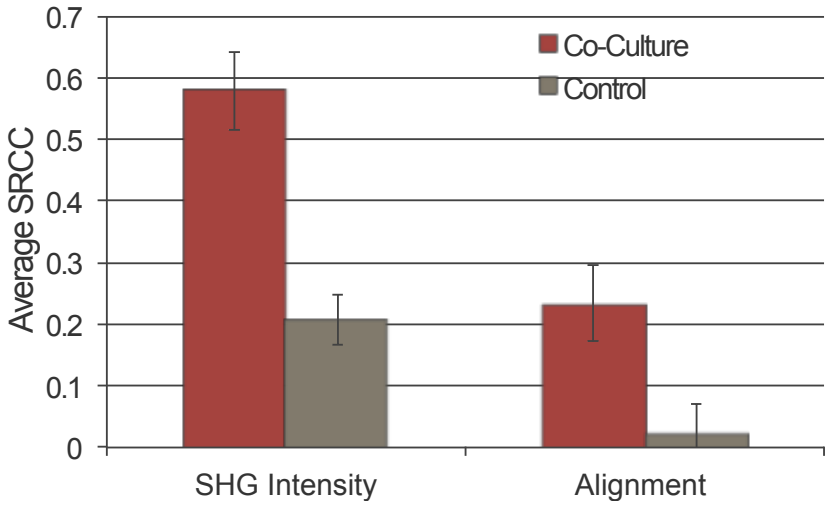

Fig. 2. Correlative Relationships Between Morphology, SHG Intensity and Collagen Fiber Alignment. Average Spearman Rank Correlation Coefficient between morphology measurement and SHG intensity (left, $p = 0.0003$) and morphology and collagen fiber alignment (right, $p = 0.0195$).

2) Inhibition of DCIS progression by blocking the activation of fibroblasts nearby MCF-DCIS cells:

After we identified the activation of stromal fibroblasts in nearby MCF-DCIS cells, we deactivated the HMFs by knocking down LRP1 in HMFs or CTSD in MCF-DCIS cells by using short-interference RNAs (siRNA). Knocking down either LRP1 or CTSD significantly reduced the number of protrusions in the HMFs and the degree of ECM alterations around them (Fig. 3). Moreover, the de-activation of HMFs efficiently inhibited the progression of DCIS to IDC (Fig. 4). The results presented here shed new insight on the phenotypic changes of fibroblasts in the vicinity of DCIS cells, suggest a strong role for this interaction in the remodeling of ECM leading to the progression from DCIS to IDC, and implicate the involvement of CTSD/LRP1 interactions in driving these changes.

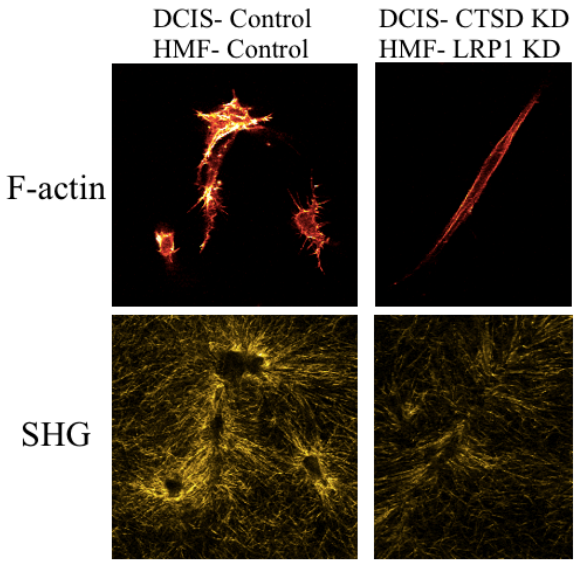

Fig. 3. Knocking down (KD) LRP1 in HMFs and CTSD in MCF-DCIS cells reduced the number of protrusions in HMFs and the degree of ECM alterations. Images showing HMFs (Red) treated with non-targeting control siRNAs (Right), and HMFs treated with LRP1-targeting siRNAs (Left). The HMFs were co-cultured with MCF-DCIS cells (control or CTSD knock-down). Corresponding SHG images (yellow) show the degree of ECM alteration around HMFs.

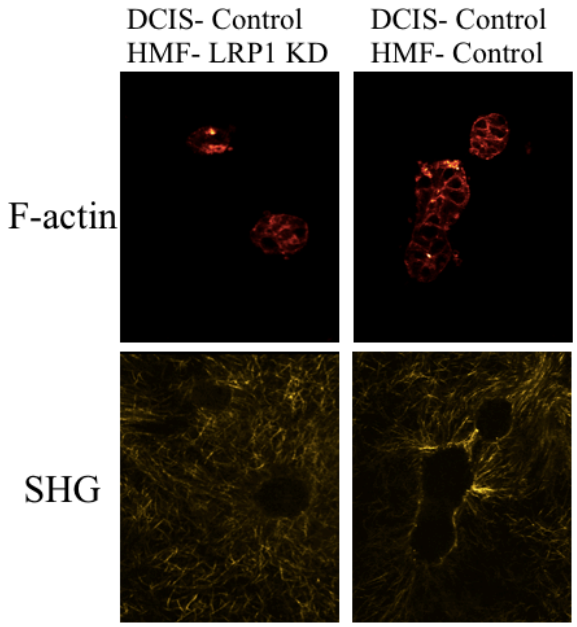

Fig. 4. Knocking down LRP1 in HMFs significantly inhibited the transition of DCIS to IDC. MCF-DCIS cells (red) co-cultured with LRP1-knock down HMFs retained rounded morphology and less ECM alteration (left). MCF-DCIS cells co-cultured with control HMFs showed elongated morphology and more ECM alterations (right).

Key research accomplishments (YR1 and YR2)

1. Microfluidic 3D compartmentalized co-culture platform was developed that enabled investigation of distance-dependent invasive transition of MCF-DCIS cells(1).
2. By using the developed microfluidic platform, we revealed that the distance between cancer cells and fibroblasts is an important factor in stimulating invasive transition of MCF-DCIS cells.
3. Heterocellular contacts between cancer cells and fibroblasts were identified as MCF-DCIS cells progressed to invasive phenotype through F-actin visualization. These contacts further stimulated the invasive transition of MCF-DCIS cells.
4. The compartmentalized microfluidic co-culture platform enabled to observe different characteristics of HMFs in the proximity to MCF-DCIS cells.

5. We verified that the signaling based on CTSD and LRP1 was necessary for the protrusive activity of stromal fibroblasts and ECM remodeling.
6. We successfully inhibited the transition of DCIS to IDC by de-activating HMFs nearby MCF-DCIS cells.
7. We found that HMFs in a 3D condition secreted a few paracrine signaling molecules such as HGF, COX2, and MMP14 at higher concentration compared to HMFs in a 2D condition, and the increased secretion of the molecules accelerated the invasive transition of MCF-DCIS cells(2).
8. We developed novel imaging analysis algorithms to quantify the morphology of fibroblasts, the protein localization within them, and the alterations in the surrounding ECM.

Reportable outcomes (YR1 and YR2)

1. Published manuscript:

- Montanez-Sauri S I, Sung K E, Berthier E, Beebe DJ, "Enabling Screening in 3D Microenvironments: Probing the Matrix and Stromal Components Effect on the Morphology and Proliferation of T47D Breast Carcinoma Cells,",*Integrative Biology*, 2013, 5, 631-640

2. *Submitted manuscripts:*

- Sung K E, Su X, Pelhke C, Berthier E, Friedl A, Beebe DJ, "Understanding the impact of 2D and 3D fibroblast cultures on in vitro breast cancer models," Submitted to *Plos One*, In revision.

3. Presentations:

- Sung K E, Pelhke C, Berthier E, Friedl A, Beebe DJ, "A micro scale in vitro model of the DCIS-IDC transition: Deciphering the role of the stroma fibroblasts", The 28th International Association for Breast Cancer Research/Breakthrough Breast Cancer Conference, Manchester, UK, 2012, Oral presentation.
- Sung K E, Pelhke C, Yang N, Eliceiri K W, Keely PJ, Friedl A, Beebe DJ, "A micro scale 3D in vitro model of the breast cancer progression from DCIS to IDC: Deciphering the role of the stromal fibroblasts", AACR Special Conference of Tumor Invasion and Metastasis, San Diego, 2013.

Conclusion

We have developed a simple compartmentalized 3D co-culture model that supports the DCIS to IDC transition in vitro(1). The model enabled us to study heterocellular-contact involved and contact-free invasive transition of MCF-DCIS cells by varying the distance between cancer and fibroblasts compartments. The ability to examine distance dependence uncovered potentially new insights about the transition to invasion suggesting the possibility of a two-step process via two different progression mechanisms: first, a soluble factor-based progression and, second, cell-cell contact signaling involved progression. During the past two years, we identified the heterocellular contact between MCF-DCIS cells and HMFs in our microfluidic co-culture system. In addition, we discovered unique properties of fibroblasts in 3D microenvironment with

MCF-DCIS cells and developed unique algorithms to efficiently analyze the alterations in cells and surrounding ECMs.

These observations were made possible by the unique functionality of the microscale model and have important implications in guiding the way we think about the transition and the development of therapeutic approaches to inhibit transition. Importantly, the simplicity of the microfluidic system enables efficient investigation of the mechanisms involved in DCIS progression and allows screening approaches to identify pathways involved. For example, the small volumes required per endpoint open the door to the use of neutralizing antibodies or siRNA approaches. The flexibility of the system will allow it to be readily adapted to create relevant in vitro 3D models for other diseases where soluble factor signaling between different cell types is important.

Appendices

Attached separately

References

1. Sung KE, Yang N, Pehlke C, Keely PJ, Eliceiri KW, Friedl A, et al. Transition to invasion in breast cancer: a microfluidic in vitro model enables examination of spatial and temporal effects. Integrative Biology. 2011 Apr 1;3(4):439–50. PMCID: PMC3094750

2. Sung KE, Su X, Berthier E, Pehlke C, Friedl A, Beebe DJ. Understanding the impact of 2D and 3D fibroblast cultures on in vitro breast cancer models. Submitted.

Personnel

David Beebe
Andreas Friedl
Kyung Eun Sung

Integrative Biology

RSC Publishing

TECHNICAL INNOVATION

View Article Online
View Journal

Cite this: DOI: 10.1039/c3ib20225a

Enabling screening in 3D microenvironments: probing matrix and stromal effects on the morphology and proliferation of T47D breast carcinoma cells†

Sara I. Montanez-Sauri,[abc] Kyung Eun Sung,[bcd] Erwin Berthier[bcd] and David J. Beebe‡*[bcd]

During breast carcinoma progression, the three-dimensional (3D) microenvironment is continuously remodeled, and changes in the composition of the extracellular matrix (ECM) occur. High throughput screening platforms have been used to decipher the complexity of the microenvironment and to identify ECM components responsible for cancer progression. However, traditional screening platforms are typically limited to two-dimensional (2D) cultures, and often exclude the influence of ECM and stromal components. In this work, a system that integrates 3-dimensional cell culture techniques with an automated microfluidic platform was used to create a new ECM screening platform that cultures cells in more physiologically relevant 3D *in vitro* microenvironments containing stromal cells and different ECM molecules. This new ECM screening platform was used to culture T47D breast carcinoma cells in mono- and co-culture with human mammary fibroblasts (HMF) with seven combinations of three different ECM proteins (collagen, fibronectin, laminin). Differences in the morphology of T47D clusters, and the proliferation of T47D cells were found in ECM compositions rich in fibronectin or laminin. In addition, an MMP enzyme activity inhibition screening showed the capabilities of the platform for small molecule screening. The platform presented in this work enables screening for the effects of matrix and stromal compositions and show promises for providing new insights in the identification of key ECM components involved in breast cancer.

Received 24th September 2012,
Accepted 10th January 2013

DOI: 10.1039/c3ib20225a

www.rsc.org/ibiology

Insight, innovation, integration

We present an innovative screening platform that integrates 3-dimensional cell culture techniques with an automated microfluidic platform to culture T47D breast carcinoma cells in more physiologically relevant 3D *in vitro* microenvironments that include different extracellular matrix (ECM) molecules and stromal fibroblasts. Traditional screening platforms are typically limited to 2-dimensional cultures, often exclude ECM molecules, stromal cells, and are less representative of the microenvironment found *in vivo*. This new microfluidic platform efficiently and effectively screens for ECM compositions within 3D microenvironments that modulate the morphology and growth of T47D cells in monocultures and co-cultures. Applying the concepts presented in this work to higher throughput screening platforms will be useful for identifying key ECM components and mechanisms involved in cancer biology.

Introduction

The mammary gland is a dynamic tissue in which cells in the mammary epithelium continuously interact with cells in the surrounding microenvironment. When the microenvironment receives signals from cells in the mammary epithelium, it sends back cues that help to maintain normal mammary tissue functions. If these interactions are disturbed, changes in the morphology, differentiation, proliferation, and migration of cells occur that can ultimately lead to the formation of a tumor and its progression to malignancy. It is believed that the major contributors to these changes are genetic alterations within the

[a] *Materials Science Program, University of Wisconsin-Madison, Madison, WI, USA*
[b] *Wisconsin Institutes for Medical Research, University of Wisconsin-Madison, Madison, WI, USA*
[c] *University of Wisconsin Carbone Cancer Center, University of Wisconsin-Madison, Madison, WI, USA*
[d] *Department of Biomedical Engineering, University of Wisconsin-Madison, Madison, WI, USA*

† Electronic supplementary information (ESI) available. See DOI: 10.1039/c3ib20225a

‡ Wisconsin Institutes for Medical Research, 1111 Highland Avenue, Room 6009, Madison, WI, 53705, USA. E-mail: djbeebe@wisc.edu; Tel: +1-608-262-2260.

epithelial cells. However, evidence shows that the extracellular matrix (ECM) composition can also influence these interactions.

The ECM is composed of different molecules with specialized properties that not only provide a physico-mechanical and geometrical scaffolding to cells, but also influence cell behavior.[1] Some of the major ECM proteins found in the mammary gland include collagens, fibronectin (FN), and laminin (LN). Type-I collagen (CN) is the major fibrillar component in the mammary gland and serves as a backbone that provides structural integrity to the mammary gland, whereas FN and LN regulate cell adhesion to the ECM. Therefore, the interactions between these ECM components and mammary epithelial cells are important for maintaining normal mammary gland tissue functions. In fact, previous studies have shown that luminal epithelial cells polarize, resemble acini structures similar to those seen *in vivo*, and express milk proteins in response to lactogenic hormones when cultured in a three-dimensional (3D), LN-rich ECM gel.[2] However, if luminal epithelial cells are cultured using traditional, 2-dimensional (2D) surfaces or CN gels lacking LN, the cells lose their polarity and their mammary-specific gene expression patterns change.[2] These results demonstrate that both the 3D microenvironment and the ECM composition play a critical role in guiding normal mammary tissue function.

During breast cancer progression, the composition of the surrounding 3D microenvironment is continuously changed and represents a major challenge for identifying specific components and/or mechanisms. Traditional 96- and 384-well plates have shown to be useful for performing high-throughput screening (HTS) toxicology assays in cancer.[3,4] However, traditional well-plate screening platforms are typically limited to the 2D culture of cells and often exclude the influence of stromal cells and ECM molecules in modulating cellular behavior of cancer cells. Fig. 1 shows some of the platforms that have been developed to address the limitations of the traditional 2D culture system. For example, three-dimensional cultures of cells in ECM proteins[5,6] have shown to be valuable tools for providing cells with a more structurally appropriate context. However, the relatively large volumes of reagents required in these assays make them more expensive and limit their throughput capabilities. Cellular microarrays have been developed to increase the throughput capacity by depositing small spots of ECM molecules on a flat surface and growing cells on the ECM spots. Cellular microarrays have shown to be useful for studying the effect of the ECM composition in the maintenance of primary rat hepatocyte phenotype, and the differentiation of mouse embryonic stem cells[7] and human mammary progenitor cells.[8] Multiple soluble formulations have also been included within cellular microarrays to examine the effect of growth factors in the growth and differentiation of embryonic stem cells.[9] However, multiple ECM spots are exposed to the same media formulation, and potential cross talk between spots can complicate the interpretation of results. Moreover, cellular microarrays are typically limited to the 2D culture of cells on top of ECM patterns, and do not represent the 3D microenvironment that is observed *in vivo*. Another approach that has been used for screening 3D cultures utilizes the hanging drop method, where spherical aggregates of cells are obtained in static or stirred suspension cultures.[10,11] The spherical aggregates have been used for testing anti-cancer drugs,[12] studying tumor cell biology,[13] and growing tumor cells and fibroblasts in co-cultures.[14] More recently, cell–polymer suspensions microinjected in collagen gels have been used to form 3D cell spheroids and visualize the distinct 3D migration of cells.[15] Although the hanging drop and microinjection methods have shown to be useful for screening monocultures and co-cultures in 3D, media is typically shared across the arrays such that results are confounded by soluble factor cross talk between array locations. Moreover, little work has been done to develop systems that include co-cultures with stromal cells as part of the 3D microenvironment. This is particularly important in breast cancer research since stromal fibroblasts play important roles in cancer development by modulating carcinoma cell proliferation both *in vivo*[16] and *in vitro*.[17] Therefore, there is a need for more biologically relevant screening platforms that provide cancer cells with 3D microenvironments rich in ECM molecules and stromal cells, while providing independent experimental conditions.

In this study, an automated ''tubeless'' microfluidic screening platform previously developed for 3D cell culture[18] was adapted to culture T47D breast carcinoma cells and human mammary fibroblasts (HMF) in 3D microenvironments and expanded to include different ECM molecules (CN, FN, LN) in the culture. The major advancements of the ECM automated microfluidic platform[18] over the previously reported 3D microfluidic platform and traditional screening platforms include the ability to culture breast carcinoma cells in 3D microenvironments of different ECM compositions, the capacity of culturing monocultures and/or co-cultures, the ability of treating cells in separate microchannels with different soluble formulations, and the potential for performing small-molecule screenings. The platform screened for ECM compositions that affect: (1) the morphology of T47D breast carcinoma clusters, (2) the proliferation of T47D breast carcinoma cells, and (3) the enzyme activity inhibition of several matrix metalloproteinases (MMP). Applying the concepts presented in this work to higher throughput screening platforms will be useful for studying cell–ECM interactions in more physiologically relevant 3D *in vitro* microenvironments, identifying specific ECM proteins, and providing new insights on key mechanisms involved in breast cancer biology.

Materials and methods

Cell culture and ECM gels preparation

The human breast carcinoma T47D cell line was generously provided by Friedl (University of Wisconsin, Madison).[21] The human mammary fibroblasts immortalized with human telomerase and labeled with GFP were provided by Kuperwasser.[22] Human T47D breast carcinoma cells were cultured in flasks with low-glucose DMEM (1.0 mg mL^{-1}, Gibco, Grand Island, NY), supplemented with 10% fetal bovine serum (FBS) and 1% penicillin/streptomycin (Invitrogen, Grand Island, NY). Human mammary fibroblasts immortalized with telomerase (HMFs)

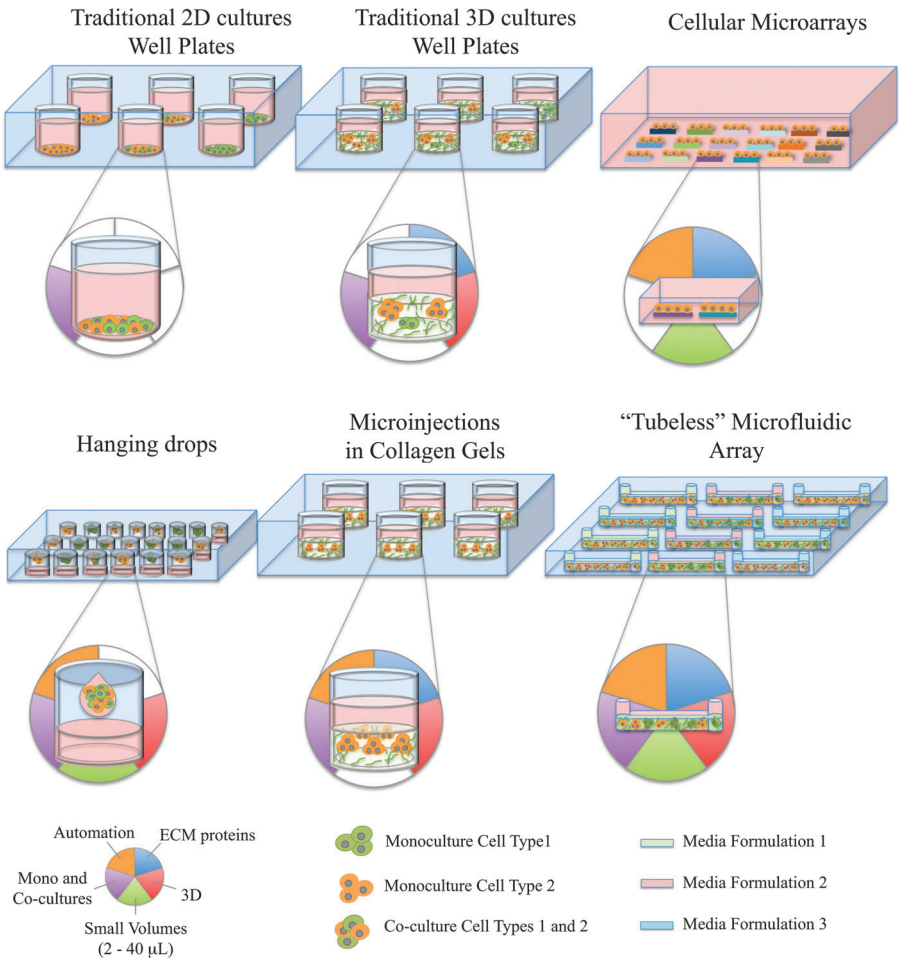

Fig. 1 Currently available screening platforms and their capabilities to include ECM proteins (blue panel), perform 3D culture (red panel), utilize small volumes of cells and reagents (green panel), include monocultures and co-cultures within a single array (purple panel), and provide a fully automated loading (orange panel). Media formulations represent the different types of soluble formulations that can be added inside separate microchannels in a microchannel array.

were cultured in high glucose DMEM (4.5 mg mL^{-1}, Gibco), supplemented with 10% calf serum (CS) and 1% penicillin/streptomycin. Both cell lines were cultured in separate flasks inside a humidified incubator at 37 °C and 5% CO_2 before mixing with ECM gels and seeding in microchannels.

Extracellular matrix gels were prepared by mixing CN with FN or LN to get a total of seven different ECM compositions. FN (1 mg mL^{-1}, human; BD Biosciences, Bedford, MA) and LN (1.88 mg mL^{-1}, mouse; BD Biosciences) were reconstituted as specified by the manufacturer. A stock solution of CN (3.64 mg mL^{-1}, rat tail; BD Biosciences) was neutralized with a solution of 100 mM HEPES buffer in 2× PBS in a 1 : 1 ratio, and incubated inside a bucket with ice for 10 minutes. Cells were re-suspended in serum-free DMEM (SF-DMEM). FN or LN were mixed with the neutralized CN, 1.5% (v/v) calf serum, and SF-DMEM to get final ECM concentrations of 1.3 mg mL^{-1} of CN with 0, 10, 50 or 100 μg mL^{-1} of FN or LN and a final cell density of 6×10^5 cells per mL (approximately 700 cells per microchannel). In co-culture experiments, HMF and T47D cells were added to the ECM gels in a 1 : 2 (HMF : T47D) ratio. 2D culture experiments were performed by coating microchannels with ECM proteins (prepared the same way as in 3D experiments) and incubating microchannels at 4 °C for 2 hours. Microchannels were rinsed with PBS three times, cells were added in the microchannels, and incubated at 37 °C afterwards. MMP activity was inhibited using the broad-spectrum inhibitor GM6001 (2.5 mM, Millipore, Billerica, MA). GM6001 was diluted in culture media and added to the gels until a final concentration of 500 nM was obtained. GM6001 was also added to cell culture media (500 nM), and cultures were replaced every other day with fresh GM6001.

Tubeless microfluidic device fabrication and automated loading

Polydimethylsiloxane (PDMS) tubeless microfluidic devices were fabricated as described previously.[18] The dimensions of the PDMS microchannels array (MCA) with straight microchannels (0.75 mm wide, 0.25 mm high, and 4.5 mm long) are shown in Fig. 2.

The automated liquid handler used to load microchannels was optimized and described previously.[18] In this work, the same platform was used to culture T47D cells in different ECM

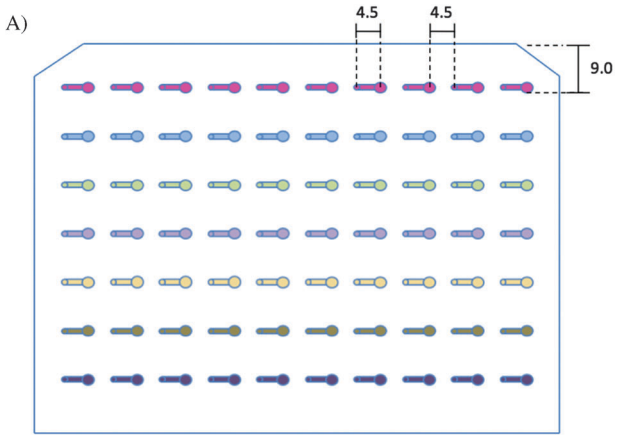

B)

Color	ECM Composition	Abbreviation
	1.3mg/mL collagen type-I	CN
	1.3mg/mL collagen type-I + 10μg/mL fibronectin	10FN
	1.3mg/mL collagen type-I + 50μg/mL fibronectin	50FN
	1.3mg/mL collagen type-I + 100μg/mL fibronectin	100FN
	1.3mg/mL collagen type-I + 10μg/mL laminin	10LN
	1.3mg/mL collagen type-I + 50μg/mL laminin	50LN
	1.3mg/mL collagen type-I + 100μg/mL laminin	100LN

Fig. 2 (A) A microchannel array was used to culture T47D cells in monocultures (first 5 microchannels per row) and in co-cultures with human mammary fibroblasts (HMF, last 5 microchannels per row) with different ECM compositions. Microchannels dimensions are shown in millimeters. (B) Seven different ECM compositions were used to culture T47D and HMF cells in the microchannel array.

compositions in the presence and absence of HMF cells. The ECM–cell mixtures were manually pipetted to seven wells of a 96-well plate and the automated platform was used to load microchannels as described previously.[18] Seven combinations of three different ECM proteins (CN, FN and LN) were used to culture T47D cells in monocultures (first 5 microchannels per row, Fig. 2A) and in co-cultures with HMF cells (last 5 microchannels per row, Fig. 2A). Between each loading with different ECM compositions, the probe was rinsed in a 50% DMSO and water solution, and washed with deionized water. The MCA included 5 replicates for each ECM–cell combination that resulted in a total of 70 microchannels. After the loading was done, the MCA was kept inside a 37 °C incubator for seven days. Media changes were done every other day. The data discussed in this work comes from at least 2 separate MCA experiments.

Immunofluorescent staining

For the quantification of T47D cluster size, cells in the MCA were stained using the automated platform as described previously.[18] T47D and HMF cells were stained with primary antibodies against pan-cytokeratin (CK, 1 : 75 dilution ratio, mouse monoclonal antihuman pan-cytokeratin; LabVision, Fremont, CA), and vimentin (VM, 1 : 150 dilution ratio, rabbit polyclonal antihuman vimentin; LabVision, Fremont, CA). Secondary antibodies were added in a 1 : 150 dilution ratio (Alexa Fluor 594 goat antimouse; Alexa Fluor 488 goat antirabbit; Invitrogen, Carlsbad, CA). For counterstaining the nuclei, Hoechst 33342 was used at 20 μg mL^{-1} (H3570; Invitrogen, Carlsbad, CA).

Image acquisition and analysis

Fluorescence imaging of T47D and HMF cells was performed on an inverted microscope (Eclipse Ti, Nikon Instruments, Melville, NY) using the NIS-Element imaging system (Diagnostic Instruments, Sterling Heights, MI). The high-throughput data analysis platform, JeXperiment (http://jexperiment.wikidot.com), was used to perform the microscopy image processing and data mining. The JeXperiment platform allowed importing data collected from each microchannel into a database, and managed the data processing for each microchannel with custom user algorithms or functions chosen from a library. Custom analysis algorithms were made to plug into the JeXperiment workflow and enabled the quantification of circularity, aspect ratio, cluster size, and total staining area of CK-positive clusters. Circularity was measured with the formula of $4\pi \times$ area per perimeter^2. Aspect ratio was defined as the ratio of major axis over minor axis. A rolling-ball background-subtraction algorithm was applied to determine a threshold value to obtain binary masks (Fig. 3). The ImageJ (Rasband, W.S., ImageJ; U.S. National Institutes of Health, Bethesda, MD, http://rsb.info.nih.gov/ij/, 1997–2009) particle analyzer was applied to obtain the circularity, aspect ratio and size of T47D clusters. The bin sizes for the cluster size histograms were determined by dividing the range of cluster sizes identified using the automated image analysis software into 7 bins. This number provided a relevant number of clusters per bin, allowing good separation between conditions while having a sufficient number of clusters in each bin. Further, the minimum (369 μm^2) and maximum (2583 μm^2) area values occurred while converting images (0.440 pixel per μm) from pixel areas (71–500 pixels) into micrometers squared. All data was analyzed using the pair-wise Wilcoxon rank sum test, and conditions significantly different ($p < 0.05$) were used in the results and discussion.

Results and discussion

The complexity of the 3D microenvironment and its constant remodeling during breast carcinoma progression represent a challenge for identifying ECM components and mechanisms involved in breast cancer. However, screening with different ECM compositions can help elucidate candidate microenvironmental components that support malignancy. An automated microfluidic platform previously developed for 3D cell culture[18] was expanded in this work to include 3D microenvironments of different ECM composition, monocultures of T47D cells, and co-cultures of T47D and HMF cells. The platform is used to treat monocultures and co-cultures separately, and to screen for the effect of the 3D ECM composition on the phenotype, behavior, and proliferation of T47D cell clusters.

Fig. 2A shows a representation of a 10 by 7 MCA used to culture T47D cells in monoculture (first 5 channels in a row) and in co-culture with HMF cells (last 5 channels in a row).

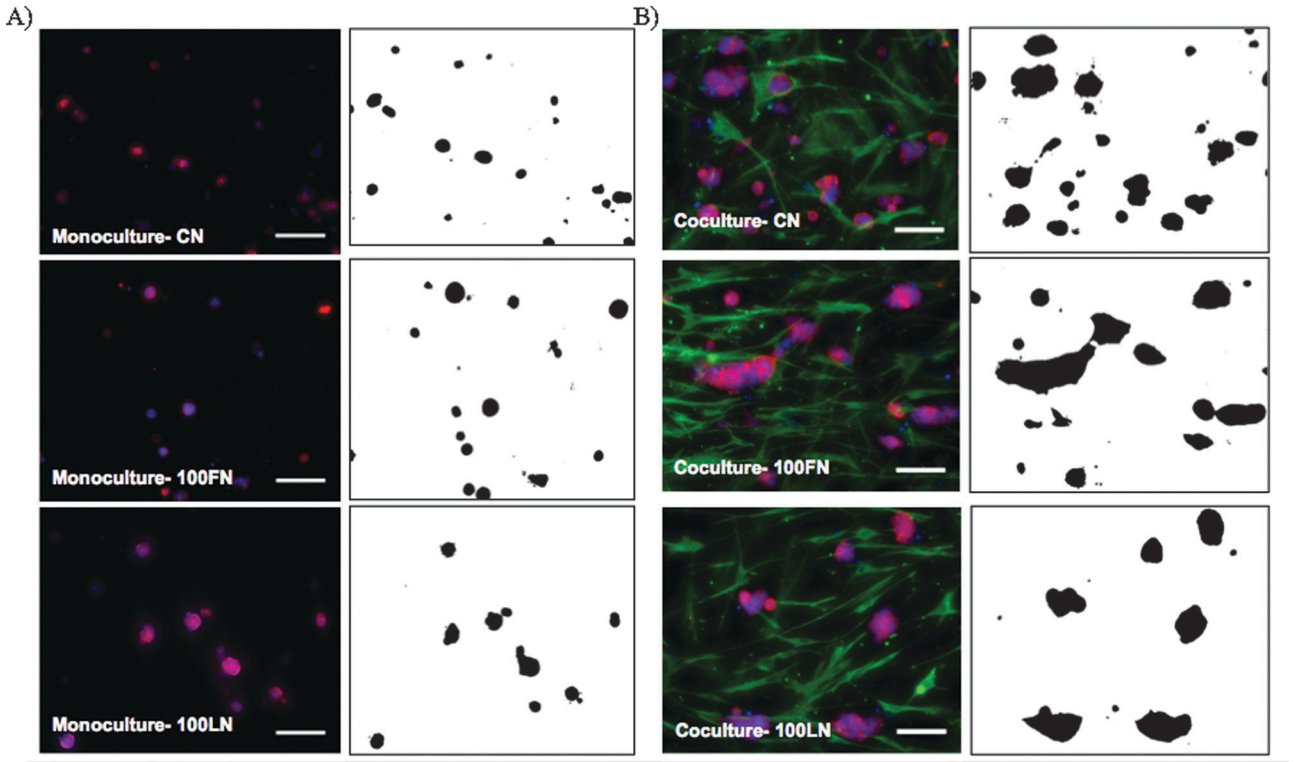

Fig. 3 Immunofluorescence images (left panels) of T47D cells in (A) monocultures, and (B) co-cultures with HMF cells inside microchannels with 1.3 mg mL^{-1} of collagen (CN), 1.3 mg mL^{-1} of collagen and 100 μg mL^{-1} of fibronectin (100FN), or 1.3 mg mL^{-1} of collagen and 100 μg mL^{-1} of laminin (100LN). Cells were cultured for 7 days, fixed, and T47D cells were stained against cytokeratin (red), HMF against vimentin (green), and nuclei with Hoechst dye (blue). Binary images (right panels) were produced with JeXperiment to analyze the morphology of T47D clusters. Scale bars represent 100 μm.

ECM compositions contained CN as the major ECM protein, and FN and LN were mixed with CN to obtain seven different ECM compositions (see Fig. 2B). Previously, the morphology[19,20] and proliferation[17,21] of breast cancer cells showed to be useful readouts to investigate breast cancer cell behavior. The total cytokeratin (CK) and nuclei staining area of T47D clusters showed a correlation with T47D cell number and have been used as readouts for T47D cell growth.[18,21] Moreover, traditional fluorescence microscopy can be used to examine T47D growth in 3D since T47D cells showed to grow evenly distributed along the horizontal and vertical dimensions of microchannels.[23] Therefore, the total staining area of T47D clusters and traditional 2D imaging are used here to examine the morphology and proliferation of T47D cell populations growing in the 3D gels.

Morphology of T47D clusters in different ECM compositions

Examining the morphology of breast cancer cells can provide important information. For example, 3D microenvironments have shown to affect the morphology and gene expression patterns of different breast cancer cell lines.[20] Also, the rigidity of the microenvironment affected the morphology of T47D cells, resulting in the down-regulation of Rho and FAK function.[24] More recently, changes in the circularity (Circ.) and aspect ratio (AR) of MCF10DCIS.com cells were used as primary readouts for studying the transition from ductal carcinoma *in situ* (DCIS) to the invasive ductal carcinoma (IDC).[19] In this work, we hypothesized that changes in the ECM composition would affect the morphology of T47D clusters. In order to test this hypothesis, the morphology of T47D clusters cultured in 3D microenvironments of different ECM compositions was examined in the presence and absence of HMF cells.

The morphology of T47D clusters was examined for different ECM compositions via immunofluorescence microscopy and binary mask image generation. Fig. 3 shows immunofluorescence images of T47D cells in monocultures (left panel, Fig. 3A), and in co-cultures with HMF cells (left panel, Fig. 3B) inside microchannels. Binary mask images (right panels, Fig. 3A and B) facilitated the automated analysis of T47D cluster morphology shown in Fig. 3. Fig. 4A and B show the circularity and aspect ratio of T47D clusters in monocultures (blue bars) and in co-cultures (red bars) with different ECM compositions. Circular clusters were defined as clusters with circularity (Circ.) or aspect ratio (AR) values close to 1. As noticed in Fig. 3A and B, in 1.3 mg mL^{-1} collagen type-I gels (CN), T47D cells formed bigger clusters in co-cultures compared to monocultures, which agreed with previously reported data.[21] However, in collagen gels containing 100 μg mL^{-1} of fibronectin (100FN), T47D clusters were bigger, but less circular (Circ. 0.48 ± 0.01, $*p < 0.02$, Fig. 4A), and more elongated (AR 2.87 ± 0.01, $*p < 0.02$, Fig. 4B) in co-cultures than in monocultures (Circ. 0.58 ± 0.02, AR 2.31 ± 0.02, Fig. 4A and B). Increasing

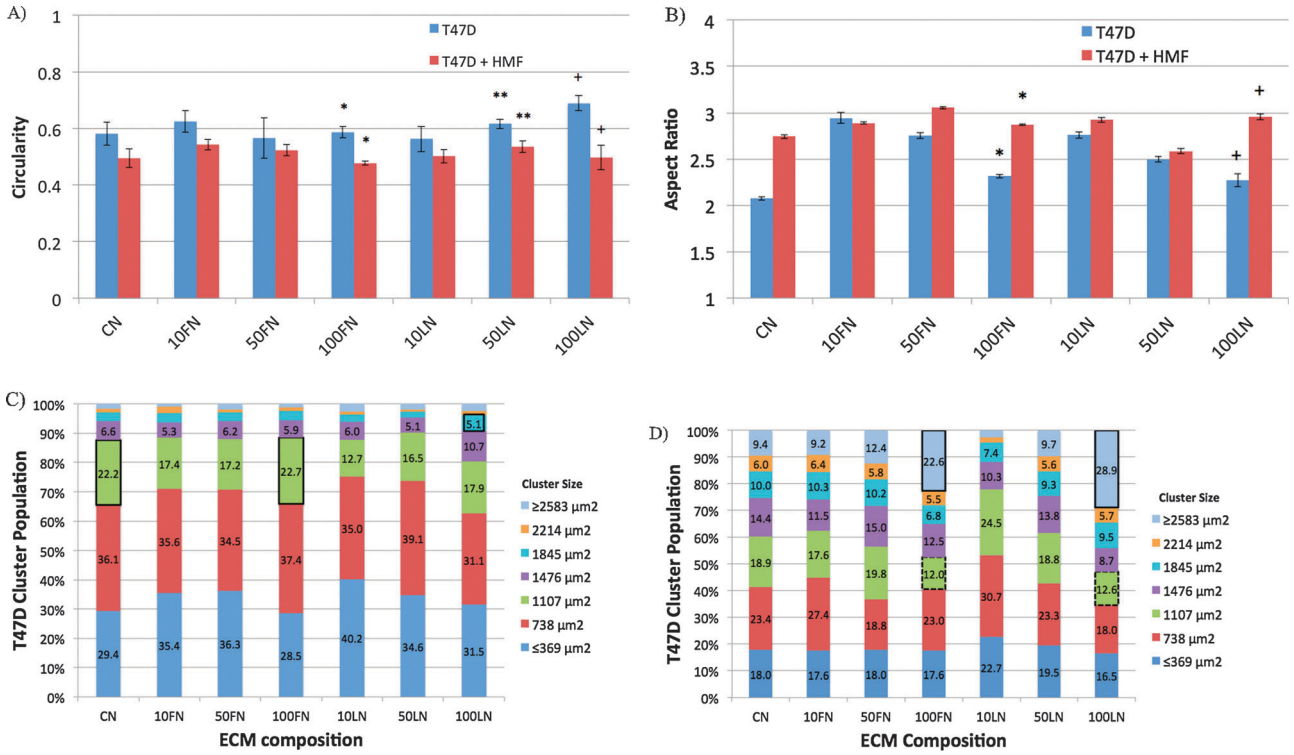

Fig. 4 The circularity (A), and aspect ratio (B) of T47D clusters were examined in monocultures (blue bars) and in co-cultures with HMF cells (red bars) for different ECM compositions after 7 days of culture inside microchannels, $*p < 0.02$, $**p < 0.05$, $+p < 0.05$, $n = 4$. T47D cluster size population was examined in monocultures (C), and in co-cultures with HMF cells (D) under the effect of different ECM compositions. Black outlined boxes represent significant increases in clusters of the same size between different ECM compositions, $p < 0.05$, $n = 4$. Black dashed lines represent significant decreases in T47D cluster size between ECM compositions of the same cluster size, $p < 0.05$, $n = 4$.

laminin concentration in collagen type-I gels (*e.g.* 100LN) also increased the circularity of clusters in monocultures (Circ. 0.69 ± 0.05, $+p < 0.05$; AR 2.27 ± 0.07, $+p < 0.02$, Fig. 4A and B) compared to co-cultures (Circ. 0.50 ± 0.04, $+p < 0.05$, AR 2.95 ± 0.03, $+p < 0.02$, Fig. 4A and B). T47D clusters in CN (Fig. 3), 10FN, 50FN, 10LN or 50LN had similar morphologies between monocultures (Fig. S1, ESI†) and co-cultures (Fig. S2, ESI†), and no significant differences were found in the circularity or aspect ratio of T47D clusters (Fig. 4A and B, $p > 0.05$). Therefore, these results show that specific ECM compositions affected the morphology of T47D clusters, and suggest that T47D clusters became more elongated when co-cultured with HMF cells at high FN or LN concentrations (*i.e.* 100FN, 50LN or 100LN).

Additionally, the size of T47D clusters was examined in monocultures and co-cultures under the influence of different ECM compositions. Fig. 4C and D show the cluster size distribution of T47D cells cultured in different ECM compositions as monocultures (Fig. 4C) or co-cultures with HMF cells (Fig. 4D). The total population of T47D clusters was divided into 7 groups (represented by different colors) that included clusters 369 μm^2 in size to 2583 μm^2. Clusters smaller than 369 μm^2 or bigger than 2583 μm^2 were also included, and statistical information about differences in cluster sizes between the different ECM compositions was analyzed (Fig. S3 and S4, ESI†). In monocultures (Fig. 4C), no significant differences were found among different ECM compositions with small (*i.e.* ≤369 to 738 μm^2) or big (2214 to ≥2583 μm^2) clusters. However, mid-sized (1107 μm^2) T47D clusters cultured with CN and 100FN displayed a modest increase in size (22.2% ± 0.2 CN, 22.7% ± 2.2 100FN, green outlined boxes, Fig. 4C) compared to other ECM compositions ($p < 0.05$ with 17.4% ± 1.0 10FN, 17.2% ± 1.0 50FN, 12.7% ± 1.8 10LN, and 16.5% ± 1.2 50LN). Similarly, 100LN also produced more clusters of size 1845 μm^2 (5.1% ± 0.8, blue outlined box, Fig. 4C) than 50LN (3.0% ± 0.6, Fig. 3C, $p < 0.05$). In co-cultures (Fig. 4D), an increase in cluster size was observed across the board, and much stronger differences between ECM compositions were found, mostly in large cluster sizes (*i.e.* 1845 μm^2 to ≥2583 μm^2, Fig. 4D). ECM compositions 100FN and 100LN displayed a depletion of mid size clusters around 1107 μm^2 (12.0% ± 1.4 100FN, 12.6% ± 3.3 100LN, $p < 0.05$, green outlined boxes, Fig. 4D), largely counterbalanced by a significant increase in the number of large clusters. For example, by increasing the concentration of FN from 10FN to 100FN, the percentage of clusters sized ≥2583 μm^2 was increased from 9.2% ± 2.1 to 22.6% ± 1.6 (blue outlined box, $p < 0.05$, Fig. 4D). The increase in the percentage of clusters larger than 2583 μm^2 was even more significant with increments of LN concentration. 10LN had only 2.5% ± 0.9 of clusters with a size of 2583 μm^2, whereas 100LN had 28.9% ± 4.3 ($p < 0.05$, blue outlined box, Fig. 4D). Moreover, the majority of clusters had a size of 738 μm^2 at low LN concentrations (*i.e.* 10LN, 30.7% ± 2.9, Fig. 4D), but as

LN concentration was increased to 100LN, the highest population of T47D clusters was shifted to 2583 μm^2 (28.9% ± 4.3, Fig. 4D).

In summary, ECM compositions containing CN, 100FN or 100LN induced an increase from small to medium size T47D clusters in monocultures. These effects were compounded in co-culture conditions, as the ECM compositions containing 100FN and 100LN induced an increase of large T47D clusters. These results show that the ECM composition affects the 3D morphology and size of T47D clusters and suggest that ECM compositions (particularly 100FN and 100LN), could impact the proliferation of T47D cells differently in monocultures and in co-cultures with HMF cells.

Proliferation of T47D cells in different ECM compositions

Measuring the proliferation of breast cancer cells has shown to be useful for predicting clinical response, providing a prognosis indicator, and studying stroma-to-carcinoma cell signaling. For example, a decrease in the proliferation index of tumor cells previously showed to be predictive of good clinical response,[25] and the proliferation of tumor cells in conjunction with tumor size, grade, nodal status, and steroid receptor status were used as useful prognostic indicators.[26] Also, a study of T47D breast carcinoma proliferation revealed that the overexpression of syndecan-1 (Sdc-1) in stromal fibroblasts stimulated T47D proliferation *in vivo*[27] and *in vitro*.[28] More recently, a co-culture system of T47D and HMF cells in 3D co-culture systems was used to decipher specific mechanisms involved in T47D growth stimulation using traditional well-plates[21] and microchannels.[29]

In this work, the culture of T47D cells was expanded with 3D microenvironments of different ECM compositions to screen for specific ECM compositions that affect T47D growth in monoculture and co-culture conditions. Fig. 5A shows the screening results for monocultures of T47D cells (blue bars) and co-cultures of T47D and HMF cells (red bars) in 3D microenvironments of different ECM compositions. As expected, co-cultures in CN supported a 2.2-fold increase in T47D cell number compared to monocultures in CN ($*p < 0.02$, Fig. 5A), which agreed with previously reported data.[18,21] In contrast, 2D cultures (cells on ECM-coated microchannels) only showed a 1.4-fold increase in T47D growth and were not able to support T47D growth as much as the 3D microenvironments ($*p < 0.05$, Fig. S5, ESI†). Moreover, most differences in T47D growth in 2D cultures were found between monocultures and co-cultures, independently of the ECM composition (Fig. S5, ESI†). On the other hand, T47D cells were more sensitive to 3D microenvironments containing FN or low concentrations of LN (*i.e.* 10LN), but not to 3D microenvironments containing 50LN or 100LN. For example, a significant decrease in CK-positive area was observed between co-cultures containing

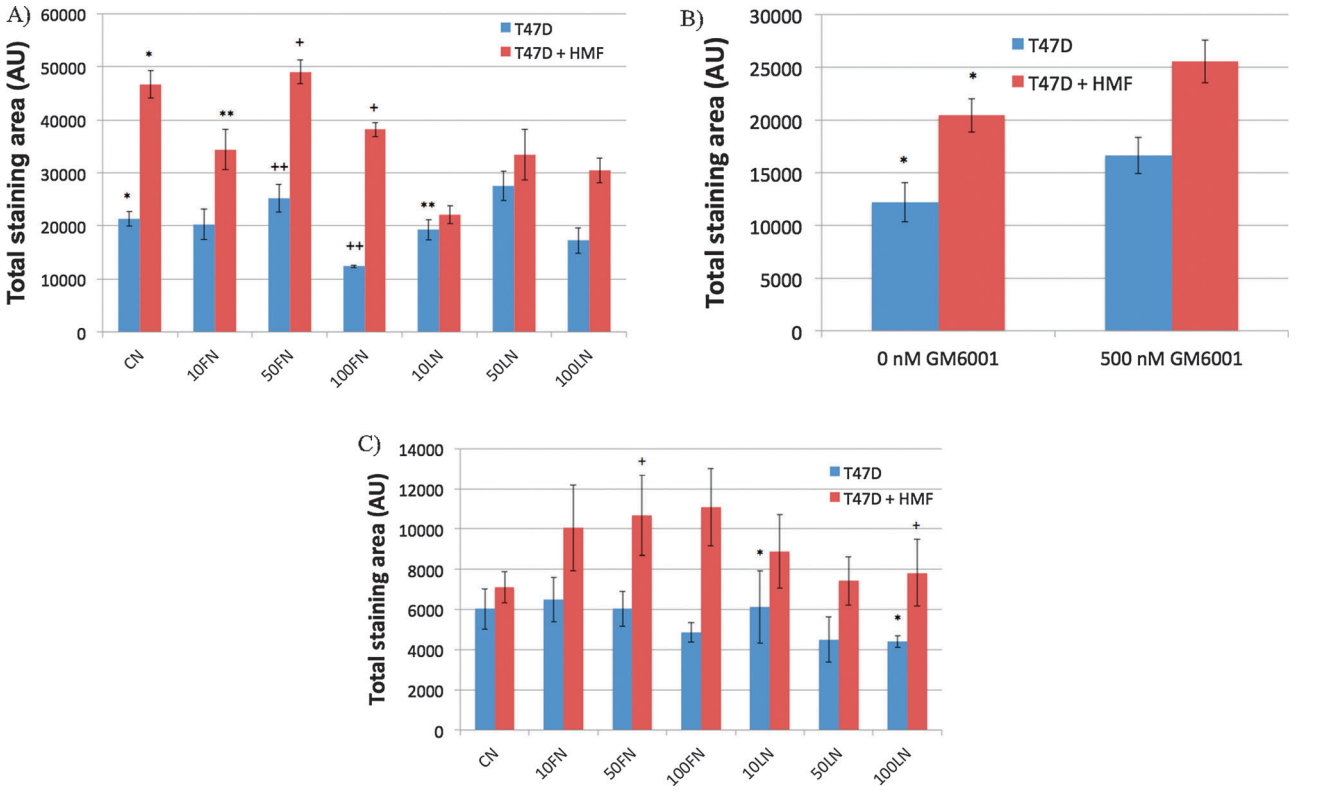

Fig. 5 The proliferation of T47D cells was analyzed after 7 days of culture in monocultures (blue bars) and co-cultures with HMF cells (red bars) in different ECM compositions. Total CK-staining area represents the total cell number of T47D cells inside microchannels. Averages were calculated from at least 4 replicates, and 2 separate experiments. (A) Screening for the influence of ECM composition in T47D proliferation. $n = 4$, $*p < 0.02$, $**p < 0.05$ compared to CN co-cultures, $+p < 0.02$, $++p < 0.02$. (B) Screening for the effect of the GM6001 MMP inhibitor in HMF-induced T47D growth in CN-only gels. $n = 5$, $*p < 0.05$. (C) Screening for the effect of the GM6001 MMP inhibitor in HMF-induced T47D growth in different ECM compositions, $n = 5$, $*p < 0.02$, $+p < 0.01$.

collagen only (CN) and samples containing 10 μg mL^{-1} of FN (10FN) or 10 μg mL^{-1} of LN (10LN) (**$p < 0.05$, Fig. 5A). Interestingly, no effect was observed between monocultures in CN, and monocultures in 10FN or 10LN. Moreover, at higher FN concentrations (*i.e.* 50FN *versus* 100FN), the growth of T47D cells was reduced in both co-cultures (+$p < 0.02$, Fig. 5A), and monocultures (++$p < 0.02$, Fig. 5A). Therefore, monocultures needed higher doses of FN (*i.e.* 100FN) in order to decrease T47D cell growth significantly, whereas in co-cultures 10FN was sufficient to decrease the growth of T47D cells. Surprisingly, an inverse effect in T47D growth was noted in 2D cultures. In 2D cultures, increasing FN concentration in monocultures also increased T47D growth (10FN *versus* 50FN, *$p < 0.04$, Fig. S5, ESI†). However, no differences were noticed in all other ECM compositions. In conclusion, 3D microenvironments influenced T47D proliferation more significantly than 2D cultures, and were able to reverse the effect of FN in 2D monocultures. In 3D microenvironments, FN affected T47D growth more than CN or LN microenvironments. These results highlight the fact that cells respond differently in 2D and 3D microenvironments, and suggest that FN could be an important ECM protein that interferes with paracrine signals between T47D and HMF cells that are necessary for supporting T47D growth.

Matrix metalloproteinase (MMP) activity inhibition in different ECM compositions

An MMP inhibitor was used to demonstrate the capability of the automated microfluidic platform to perform small molecule screenings. The broad-spectrum MMP inhibitor GM6001 was previously used to abolish HMF-induced T47D growth in CN-only gels.[29] In this study, the inhibition of HMF-induced T47D growth was screened for different ECM compositions in monocultures and in co-cultures with HMF cells. GM6001 (500 nM) was added to the gels and to the cell culture medium, and GM6001-containing samples were loaded in the MCA. Fig. 5B shows the total CK staining area of T47D cells cultured inside microchannels as monocultures (blue bars) or co-cultures with HMF cells (red bars) in CN-only gels. A significant increase in T47D growth was observed in co-cultures of T47D and HMF cells compared to T47D monocultures (*$p < 0.05$, Fig. 5B) when the inhibitor GM6001 was not added. However, no significant differences were found between monocultures and co-cultures in the presence of GM6001, which agreed with data reported previously.[29]

Fig. 5C shows the effect of the MMP enzyme activity inhibitor in different ECM compositions. As expected, the stimulation of T47D cell growth by HMF cells was blocked in CN samples, and no significant differences were observed between monocultures and co-cultures (Fig. 5C). Moreover, the increase of T47D cell growth by HMF cells was blocked by GM6001 in all the ECM compositions tested. This indicated that MMP activity was dominant over ECM composition to support breast cancer cell growth. However, in monocultures, 10LN supported T47D cell growth better than 100LN (*$p < 0.05$, Fig. 5C), and in co-cultures, FN increased T47D cell growth more significantly than compositions containing LN (*e.g.* 50FN *versus* 100LN, +$p < 0.02$, Fig. 5C). Therefore, although the ECM composition did not affect the growth of T47D cells between monocultures and co-cultures, significant differences in the growth of T47D cells within monocultures or co-cultures show that the ECM composition influences T47D growth even in the presence of a MMP inhibitor.

Conclusion

An automated microfludic platform for 3D cell culture[18] was expanded in this work to culture cells in 3D microenvironments of different ECM compositions, and to screen for ECM compositions that influenced the morphology of T47D clusters, the proliferation of T47D cells, and the effect of a broad-spectrum MMP inhibitor in T47D growth. The morphology quantification revealed ECM-specific differences (particularly in 100FN and 100LN) in the circularity of T47D clusters between monocultures and co-cultures. Also, differences in the size-distribution of T47D clusters were found within co-cultures in CN and co-cultures containing 100FN or 100LN. These results suggested a compounded effect of the ECM composition and culture conditions on the proliferation of T47D cells. In fact, a proliferation screening showed that T47D cell growth decreased only in co-cultures containing 10 μg mL^{-1} of FN (10FN condition) and not in monocultures. Moreover, 3D microenvironments influenced T47D growth more significantly than 2D cultures, thus highlighting the importance of the 3D microenvironment. Finally, an MMP inhibition screening showed that although blocking the MMP activity reduced the growth of T47D cells in co-cultures in all the ECM compositions tested, FN still supported T47D growth better than LN.

The microfluidic platform presented in this work provides an information-rich *in vitro* assay that presents many advantages over current ECM screening platforms. First, culturing cells embedded in 3D microenvironments rich in both stromal cells and ECM molecules increased the biological relevance of the screening. Second, the small volumes of ECM proteins and cells required for loading each microchannel (approximately 2 μL per microchannel) allows for a cost-effective screening of ECM compositions when compared to the volumes required in traditional 3D cell culture assays (approximately 50 μL per well). Third, the enclosed compartments provided by microchannels allowed the individualized treatment of monocultures and co-cultures within a single MCA, and the analysis of paracrine interactions between T47D and HMF cells. Finally, an MMP inhibitor screening showed the capability of the platform to perform small molecule inhibitor screenings.

This new platform promises to be useful for advancing the development of more *in vivo*-like screening platforms. For example, screening in 3D cultures can provide relevant information about the performance of cancer drugs by using more biologically relevant 3D cultures. Also, the reduced amount of reagents required in this platform, and its ability to culture and treat cells in separate compartments can be expanded to incorporate different cancer cell lines (normal and malignant), primary cells, ECM molecules, and soluble formulations. Defined microenvironmental compositions within the MCA will also expedite the identification of important ECM molecules

and mechanisms involved in cancer. Finally, increasing the number of microchannels in the MCA will provide a higher throughput analysis to further study the role of ECM and stromal components, and identify new drug targets in breast cancer.

Acknowledgements

This work was supported by the NIH grants R33CA137673, DOD/BRCP W81XWH-11-1-0208, DOD BCRP W81XWH-10-BCRP-CA, KRF-2008-220-D00133 and NLM5T15LM007359.

References

1 A. Lochter and M. J. Bissell, Involvement of extracellular-matrix constituents in breast-cancer, *Semin. Cancer Biol.*, 1995, **6**(3), 165–173.
2 M. H. Barcellos-Hoff, J. Aggeler, T. G. Ram and M. J. Bissell, Functional differentiation and alveolar morphogenesis of primary mammary cultures on reconstituted basement membrane, *Development*, 1989, **105**(2), 223–235.
3 H. Mueller, M. U. Kassack and M. Wiese, Comparison of the usefulness of the MTT, ATP, and calcein assays to predict the potency of cytotoxic agents in various human cancer cell lines, *J. Biomol. Screening*, 2004, **9**(6), 506–515.
4 S. Kasibhatla, H. Gourdeau, K. Meerovitch, J. Drewe, S. Reddy, L. Oiu, H. Zhang, F. Bergeron, D. Bouffard, Q. Yang, J. Herich, S. Lamothe, S. X. Cai and B. Tseng, Discovery and mechanism of action of a novel series of apoptosis inducers with potential vascular targeting activity, *Mol. Cancer Ther.*, 2004, **3**(11), 1365–1373.
5 J. Debnath and J. S. Brugge, Modelling glandular epithelial cancers in three-dimensional cultures, *Nat. Rev. Cancer*, 2005, **5**(9), 675–688.
6 G. Y. Lee, P. A. Kenny, E. H. Lee and M. J. Bissell, Three-dimensional culture models of normal and malignant breast epithelial cells, *Nat. Methods*, 2007, **4**(4), 359–365.
7 C. J. Flaim, S. Chien and S. N. Bhatia, An extracellular matrix microarray for probing cellular differentiation, *Nat. Methods*, 2005, **2**(2), 119–125.
8 M. A. LaBarge, C. M. Nelson, R. Villadsen, A. Fridriksdottir, J. R. Ruth, M. R. Stampfer, O. W. Petersen and M. J. Bissell, Human mammary progenitor cell fate decisions are products of interactions with combinatorial microenvironments, *Integr. Biol.*, 2009, **1**(1), 70–79.
9 C. J. Flaim, D. Teng, S. Chien and S. N. Bhatia, Combinatorial signaling microenvironments for studying stem cell fate, *Stem Cells Dev.*, 2008, **17**(1), 29–39.
10 L. A. Kunz-Schughart, J. P. Freyer, F. Hofstaedter and R. Ebner, The use of 3-D cultures for high-throughput screening: The multicellular spheroid model, *J. Biomol. Screening*, 2004, **9**(4), 273–285.
11 F. Hirschhaeuser, H. Menne, C. Dittfeld, J. West, W. Mueller-Klieser and L. A. Kunz-Schughart, Multicellular tumor spheroids: An underestimated tool is catching up again, *J. Biotechnol.*, 2010, **148**(1), 3–15.
12 Y. C. Tung, A. Y. Hsiao, S. G. Allen, Y. S. Torisawa, M. Ho and S. Takayama, High-throughput 3D spheroid culture and drug testing using a 384 hanging drop array, *Analyst*, 2011, **136**(3), 473–478.
13 L. A. Kunz-Schughart, M. Kreutz and R. Knuechel, Multicellular spheroids: a three-dimensional *in vitro* culture system to study tumour biology, *Int. J. Exp. Pathol.*, 1998, **79**(1), 1–23.
14 T. K. Hoffmann, K. Schirlau, E. Sonkoly, S. Brandau, S. Lang, A. Pivarcsi, V. Balz, A. Muller, B. Homey, E. Boelke, T. Reichert, U. Friebe-Hoffmann, J. Greve, P. Schuler, K. Scheckenbach, J. Schipper, M. Bas, T. L. Whiteside and H. Bier, A novel mechanism for anti-EGFR antibody action involves chemokine-mediated leukocyte infiltration, *Int. J. Cancer*, 2009, **124**(11), 2589–2596.
15 H. H. Truong, J. de Sonneville, V. P. S. Ghotra, J. L. Xiong, L. Price, P. C. W. Hogendoorn, H. H. Spaink, B. van de Water and E. H. J. Danen, Automated microinjection of cell-polymer suspensions in 3D ECM scaffolds for high-throughput quantitative cancer invasion screens, *Biomaterials*, 2012, **33**(1), 181–188.
16 D. Broutyboye and H. Raux, Differential Influence of Stromal Fibroblasts from Different Breast Tissues on Human Breast-Tumor Cell-Growth in Nude-Mice, *Anticancer Res.*, 1993, **13**(4), 1087–1090.
17 A. Sadlonova, Z. Novak, M. R. Johnson, D. B. Bowe, S. R. Gault, G. P. Page, J. V. Thottassery, D. R. Welch and A. R. Frost, Breast fibroblasts modulate epithelial cell proliferation in three-dimensional *in vitro* co-culture, *Breast Cancer Res.*, 2005, **7**(1), R46–R59.
18 S. I. Montanez-Sauri, K. E. Sung, J. P. Puccinelli, C. Pehlke and D. J. Beebe, Automation of three-dimensional cell culture in arrayed microfluidic devices, *J. Lab. Autom.*, 2011, **16**(3), 171–185.
19 K. E. Sung, N. Yang, C. Pehlke, P. J. Keely, K. W. Eliceiri, A. Friedl and D. J. Beebe, Transition to invasion in breast cancer: a microfluidic *in vitro* model enables examination of spatial and temporal effects, *Integr. Biol.*, 2011, **3**(4), 439–450.
20 P. A. Kenny, G. Y. Lee, C. A. Myers, R. M. Neve, J. R. Semeiks, P. T. Spellman, K. Lorenz, E. H. Lee, M. H. Barcellos-Hoff, O. W. Petersen, J. W. Gray and M. J. Bissell, The morphologies of breast cancer cell lines in three-dimensional assays correlate with their profiles of gene expression, *Mol. Oncol.*, 2007, **1**(1), 84–96.
21 G. Su, S. A. Blaine, D. H. Qiao and A. Friedl, Shedding of syndecan-1 by stromal fibroblasts stimulates human breast cancer cell proliferation *via* FGF2 activation, *J. Biol. Chem.*, 2007, **282**(20), 14906–14915.
22 C. Kuperwasser, T. Chavarria, M. Wu, G. Magrane, J. W. Gray, L. Carey, A. Richardson and R. A. Weinberg, Reconstruction of functionally normal and malignant human breast tissues in mice, *Proc. Natl. Acad. Sci. U. S. A.*, 2004, **101**(14), 4966–4971.
23 G. Su, K. E. Sung, D. J. Beebe and A. Friedl, Functional screen of paracrine signals in breast carcinoma fibroblasts, *PLoS One*, 2012, **7**(10), e46685.
24 M. A. Wozniak, R. Desai, P. A. Solski, C. J. Der and P. J. Keely, ROCK-generated contractility regulates breast

epithelial cell differentiation in response to the physical properties of a three-dimensional collagen matrix, *J. Cell Biol.*, 2003, **163**(3), 583–595.

25 J. Chang, T. J. Powles, D. C. Allred, S. E. Ashey, G. M. Clark, A. Makris, L. Assersohn, R. K. Gregory, C. K. Osborne and M. Dowsett, Biologic markers as predictors of clinical outcome from systemic therapy for primary operable breast cancer, *J. Clin. Oncol.*, 1999, **17**(10), 3058–3063.

26 M. J. Beresford, G. D. Wilson and A. Makris, Measuring proliferation in breast cancer: practicalities and applications, *Breast Cancer Res.*, 2006, **8**(6), 216.

27 T. Maeda, J. Desouky and A. Friedl, Syndecan-1 expression by stromal fibroblasts promotes breast carcinoma growth *in vivo* and stimulates tumor angiogenesis, *Oncogene*, 2006, **25**(9), 1408–1412.

28 T. Maeda, C. M. Alexander and A. Friedl, Induction of syndecan-1 expression in stromal fibroblasts promotes proliferation of human breast cancer cells, *Cancer Res.*, 2004, **64**(2), 612–621.

29 M. Bauer, G. Su, D. J. Beebe and A. Friedl, 3D microchannel co-culture: method and biological validation, *Integr. Biol.*, 2010, **2**(7–8), 371–378.

PLOS ONE

Understanding the impact of 2D and 3D fibroblast cultures on in vitro breast cancer models

--Manuscript Draft--

Manuscript Number:	PONE-D-13-06531
Article Type:	Research Article
Full Title:	Understanding the impact of 2D and 3D fibroblast cultures on in vitro breast cancer models
Short Title:	The impact of 3D culture on breast cancer model
Corresponding Author:	David Beebe University of Wisconsin - Madison UNITED STATES
Keywords:	3D in vitro system; Breast cancer progression; microfluidics; extracellular matrix; Tumor-stroma interaction
Abstract:	The utilization of 3D, physiologically relevant in vitro cancer models to investigate complex interactions between tumor and stroma has been increasing. Prior work has generally focused on the cancer cells and, the role of fibroblast culture conditions on tumor-stromal cell interactions is still largely unknown. Here, we focus on the stroma by comparing functional behaviors of human mammary fibroblasts (HMFs) cultured in 2D and 3D and their effects on the invasive progression of breast cancer cells (MCF10DCIS.com). We identified increased levels of several paracrine factors from HMFs cultured in 3D conditions that drive the invasive transition. Using a microscale co-culture model with improved compartmentalization and sensitivity, we demonstrated that HMFs cultured in 3D intensify the promotion of the invasive progression through the HGF/c-Met interaction. This study highlights the importance of the 3D stromal microenvironment in the development of multiple cell type in vitro cancer models.
Order of Authors:	Kyung E Sung
	Xiaojing Su
	Erwin Berthier
	Carolyn Pehlke
	Andreas Friedl
	David Beebe
Suggested Reviewers:	Claudia Fischbach-Teschl Cornell University cf99@cornell.edu Dr. Fischbach conducts multidisciplinary research across fields such as 3D biology and micro in vitro systems. Dr. Fischbach has many publications about designing appropriate 3D in vitro systems to gain better qualitative and quantitative understanding of microenvironmental conditions in cancer. Therefore, we believe that Dr. Fischbach could provide fair comments on our manuscript.
	Mina J Bissell Lawrence Berkeley National Laboratory mjbissell@lbl.gov Dr. Bissell is a distinguished scientist in breast cancer research, particularly regarding 3D tumor microenvironments. One of Dr. Bissell's research foci is the role of extracellular matrices in malignant breast tissue. As our manuscript demonstrates the impact of 3D in vitro systems in investigating breast cancer progression, we believe that Dr. Bissell could provide valuable comments on our manuscript.
Opposed Reviewers:	

January 11, 2013

Editor, *PLOS ONE*

I am enclosing a manuscript titled "Understanding the impact of 2D and 3D fibroblast cultures on *in vitro* breast cancer models," co-authored with K.E. Sung, X. Su, E. Berthier, C. Pehlke, A. Friedl which we are submitting to *PLOS ONE* for possible publication as an Article.

While the importance of the microenvironment is increasingly evident, there is still surprisingly few studies that directly compare 2D vs 3D culture in the context of cancer progression. Here we perform such comparisons within the specific context of the transition from ductal carcinoma in situ (DCIS) to invasive ductal carcinoma (IDC) in breast cancer. Our data underscores the importance of 3D *in vitro* systems in paracrine interactions and identifies important factors that influence breast cancer progression from DCIS to IDC by directly comparing functional behaviors of human mammary fibroblasts (HMF) cultured in 2D and 3D conditions. One of our major findings was that HMFs in 3D culture produced a a few fold increase in hepatocyte growth factor (HGF) concentrations as compared to HMFs in 2D culture. We also found that because of this increased HGF secretion, HMFs in 3D culture cause a more accelerated transition to IDC compared to 2D conditions. We also advanced *in vitro* system technology by developing a compartmentalized microfluidic *in vitro* platform that allows combined 3D and 2D co-cultures. This microfluidic system possesses several advantages over traditional co-culture systems. For example, our system facilitates simultaneous monitoring of each cell compartment and reduces the number of cells and ECM proteins required. This study will appeal to the diverse readership of *PLOS ONE* because it presents intriguing findings relevant to the role the microenvironment plays in breast cancer progression and also presents technological advances in designing *in vitro* models.

Suggested academic editors of this manuscript include:
1) Professor Edna Cukierman: Cancer Biology Program, Fox Chase Cancer Center, Email: Edna.Cukierman@fccc.edu, Office Phone: +1-215-214-4218
2) Professor Sanjay Kumar: Department of Bioengineering, UC Berkeley, Email: skumar@berkeley.edu, Office Phone: +1-510-643-0787

Recommended reviewers of this manuscript include:
1) Professor Claudia Fischbach-Teschl: Department of Biomedical Engineering, Cornell University, Email: cf99@cornell.edu, Office Phone: +1-607-255-4547
2) Professor David J. Mooney: Department of Bioengineering, Harvard Engineering & Applied Science, Email: mooneyd@seas.harvard.edu, Office Phone: +1-617-495-8624
3) Professor Mina J. Bissell: Cancer & DNA Damage Responses Department, Life Science Division, Lawrence Berkeley National Laboratory, Email: mjbissell@lbl.gov, Office Phone: +1-510-486-4365
4) Professor Philip R. LeDuc: Department of Mechanical Engineering, Carnegie Mellon University, Email: prl@andrew.cmu.edu, Office Phone: +1-412-268-2504

Please contact me if I can provide additional information about our manuscript. Thank you for considering it for possible publication.

Sincerely,

David J. Beebe
Professor
Department of Biomedical Engineering
Wisconsin Institute for Medical Research
University of Wisconsin
1111 Highland Ave.
Madison, WI 53705
Email: djbeebe@wisc.edu

Understanding the impact of 2D and 3D fibroblast cultures on in vitro breast cancer models

Kyung Eun Sung[1,4,5], Xiaojing Su[1,4], Erwin Berthier[2], Carolyn Pehlke[1,4,5], Andreas Friedl[3,4,5], David J. Beebe[1,4,5]*

[1]Department of Biomedical Engineering, [2]Department of Medical Microbiology, [3]Department of Pathology and Laboratory Medicine, [4]Paul P. Carbone Comprehensive Cancer Center, [5]Laboratory of Optical and Computational Instrumentation, University of Wisconsin, Madison, WI, USA

* Corresponding author:

David J. Beebe

Department of Biomedical Engineering

Wisconsin Institute for Medical Research

University of Wisconsin

1111 Highland Ave.

Madison, WI 53705

Email: djbeebe@wisc.edu

Abstract

The utilization of 3D, physiologically relevant in vitro cancer models to investigate complex interactions between tumor and stroma has been increasing. Prior work has generally focused on the cancer cells and, the role of fibroblast culture conditions on tumor-stromal cell interactions is still largely unknown. Here, we focus on the stroma by comparing functional behaviors of human mammary fibroblasts (HMFs) cultured in 2D and 3D and their effects on the invasive progression of breast cancer cells (MCF10DCIS.com). We identified increased levels of several paracrine factors from HMFs cultured in 3D conditions that drive the invasive transition. Using a microscale co-culture model with improved compartmentalization and sensitivity, we demonstrated that HMFs cultured in 3D intensify the promotion of the invasive progression through the HGF/c-Met interaction. This study highlights the importance of the 3D stromal microenvironment in the development of multiple cell type in vitro cancer models.

Introduction

Cancer cells cultured in an extra cellular matrix (ECM) (often called three-dimensional (3D) culture) show differences in functional behaviors such as differentiation, proliferation, and gene expression[1-3], when compared to cells cultured on a flat surface (two-dimensional (2D)). The growing consensus is that 3D models recreate key aspects of the microenvironment more faithfully and, in some cases, provide more

comprehensive and relevant biological information that is impossible or difficult to obtain from 2D models[4-6]. This realization has prompted increased use and exploitation of 3D culture for in vitro cancer models[3,7-9]. One hypothesis attributes the changes observed in 3D culture to the enhanced interactions between c3ells and the surrounding ECM. This hypothesis is supported by reports of a growing number of different signaling mechanisms in 3D microenvironments compared to 2D microenvironments over the last decade[7,9-12]. However, there are still relatively few studies directly comparing 2D vs. 3D in vitro systems. In addition, while the role of the matrix in regulating fibroblast behavior has been previously studied, the consequences of modified fibroblast behavior via paracrine signaling with cancer cells is less well understood. Co-culture of cancerous cells with stromal fibroblasts has been shown to induce significant changes in tumor development and progression. Fibroblasts surrounding a pre-invasive tumor can become activated and play a critical role in the progression to invasion via enhanced secretion of cytokines, growth factors, and proteases such as TGFβ1, HGF, SDF-1, and MMP2[13-15]. Particularly in breast cancer, the progression from ductal carcinoma in situ (DCIS) to invasive ductal carcinoma (IDC) is believed to be actively driven by complex interactions with the surrounding microenvironment including interactions with various stromal fibroblasts[16-20]. In this study, we focus on examining the paracrine interaction between cancer cells and stromal fibroblasts during the breast cancer progression from DCIS to IDC in the context of matrix effects on the stromal cells and their subsequent regulation of cancer progression.

To obtain a more comprehensive understanding of the complex tumor-stroma interactions during breast cancer progression, it is critical to develop a more holistic view of the effect of the microenvironment on the interaction between multiple cell types. Current studies, based on platforms such as the transwell or multiwell assay, focus primarily on the tumor cell, while neglecting to consider the culture environment of the co-cultured fibroblast cells. Further, these models have limited functionality when investigating more complex mechanisms including paracrine/autocrine signaling, cell-cell physical interactions, and matrix-cell interactions. Microfluidic models have been shown to provide a higher level of control over the microenvironment, noticeably through the ability to control ECM and soluble-factor signaling cues separately[21-26]. For example, we recently developed an in vitro co-culture model of stromal and cancer cells that supports the progression from DCIS to IDC using a simple microfluidic system[27]. Importantly, the microfluidic system is capable of mimicking the microenvironment more precisely than conventional systems enabling lines of inquiry that are difficult to pursue using traditional systems. To date, however, the conditions of stromal fibroblast culture are rarely considered in these models, and, to the best of our knowledge, have not been mechanistically well assessed.

In this study, we examined the influence of 2D and 3D culture of human mammary fibroblasts (HMFs) on the invasive transition of breast cancer cells (MCF10-DCIS.com (MCF-DCIS) cells), specifically known as the DCIS to IDC transition. We show that when HMFs are cultured in a 3D matrix, they secrete more paracrine signaling molecules than in 2D culture conditions and that these molecules increase the

invasive behavior in DCIS cells. First, we collected conditioned media from 2D and 3D cultures of HMFs and measured the degree of invasive transition of MCF-DCIS cells in the different conditioned media. Second, we analyzed the mRNA expression of five stromal fibroblast-derived molecules (CXCL12, MMP14, HGF, COX2, and TGFβ1) of HMFs cultured in 2D and 3D conditions. Bead-based ELISA was performed to profile the concentrations of eight secreted proteins in 2D and 3D conditions. Among the examined molecules, HGF was selected for further investigation because of its known effect in the invasion of cancer cells, particularly through its ability to activate c-Met. HGF/c-Met signaling was further validated by adding a neutralizing antibody against HGF and a small molecule inhibitor that inhibits c-Met phosphorylation. Finally, we developed and applied a 3D microfluidic platform to perform 3D and 2D combined co-culture of MCF-DCIS cells and HMFs to validate the data obtained in the conditioned media experiments using a more holistic model. This work underscores the importance of a 3D microenvironment in paracrine interactions, identifies important factors that influence progression and whose expression is increased in 3D culture and validates micro culture models as a useful tool enabling advanced studies.

Results and Discussion

MCF-DCIS cells show the ability to replicate key aspects of breast cancer progression from DCIS to IDC[16,28,29]. This transition has further been shown to be facilitated by co-culture with fibroblasts, particularly when fibroblasts are cultured in 3D conditions versus 2D conditions[27]. Here, we propose a mechanistic assessment of the effects

of 2D and 3D culture conditions on the functional activity of HMFs and their subsequent impact on the invasive transition of MCF-DCIS cells using both established macroscale methods and emerging microscale methods.

HMFs cultured in 3D induce a more invasive transition of MCF-DCIS cells than HMFs cultured in 2D conditions.

We first assessed functional differences of HMFs cultured in 2D and 3D conditions by comparing the amount of secreted signaling molecules from HMFs present in culture media. Further, the effect of HMFs cultured in 2D and 3D conditions on the invasive transition of MCF-DCIS cells was investigated. To examine effects solely caused by soluble molecules in each condition, conditioned media from 2D and 3D cultures of HMFs was collected after 48 hours of culture in 48 well-plates and added to 3D cultures of MCF-DCIS cells in 48 well-plates (Fig. 1a). The transition of MCIS-DCIS cells to an invasive phenotype was evaluated using two well-established measures: the aspect ratio (AR, major axis over minor axis) and the degree of invasion in transwells. Conditioned media from HMF cultured in 3D induced a more invasive transition of MCF-DCIS cells (Fig. 1b), which displayed more elongated clusters (i.e., higher aspect ratio). Additionally, transwell invasion assays showed a higher invasion of MCF-DCIS cells when stimulated by 3D conditioned media than by 2D conditioned media ($p=0.022$) (Fig. 1c). To exclude any potential effects of Matrigel, which contains various soluble factors, the same experiments were performed with a collagen I pure matrix, and a similar trend was observed (data not shown). These observations

suggest that increased secretions of specific signaling molecules from fibroblasts occur in 3D conditions, and these stimulate the invasive transition of MCF-DCIS cells.

To identify which molecules are secreted at higher concentrations in 3D conditions, we analyzed 1) mRNA levels, 2) gelatinase (MMP2 and MMP9) activity, and 3) concentrations of secreted proteins from HMFs cultured in 2D vs. 3D. First, mRNA expression of five selected molecules (HGF, COX2, MMP14, TGFβ1, and CXCL12) in HMFs cultured in 2D and 3D conditions were quantified after 48 hours cultivation in each condition. Because HMFs proliferate faster under 2D conditions, 2D samples were loaded at a lower density in order to acheive similar final cell densities as compared to the 3D samples at the collection time (48 hours) (Supplementary Fig. 1). This proliferation difference is consistent with a previous study led by Su et al[30]. Among the five molecules tested, HGF, MMP14, and COX2 showed higher expression from HMFs cultured in 3D conditions compared to HMFs cultured in 2D conditions. CXCL12 showed an opposite trend (Fig. 2b). TGFβ1 expression levels were not significantly different between HMFs cultured in 2D and 3D conditions. Second, using zymography, we found that active MMP2 secretion was higher in HMFs cultured in 3D conditions, and MMP9 was not detectable in either 2D or 3D conditions (Fig. 2c). We examined the effect of different gel densities on 3D conditions by testing a range of gel densities and proliferation effects (since 2D conditions induce increased cell growth) by testing different cell seeding densities. All of these conditions displayed similar trends (Supplementary Fig. 1). As no significant differences were observed for the different cell and collagen densities tested, we chose a high cell density for the 2D

conditions ($6x10^4$cells/well) and a lower concentration of the 3D mixed matrix (50:50 Matrigel:collagen I, the final concentration of collagen I — 0.8mg/ml) for all subsequent experiments.

Finally, bead-based ELISA was used to quantify the concentrations of eight secreted proteins (HGF, IL6, IL8, FGF2, TNFα, TGFα, TGFβ1, VEGF) from HMFs as well as from MCF-DCIS cells in 2D compared to 3D. The results showed that seven molecules (out of eight) were secreted in higher concentrations from HMFs in 3D than in 2D (Fig. 2d, raw data are shown in Supplementary Fig. 3). MCF-DCIS cells, on the other hand, secreted relatively similar amounts of the eight proteins analyzed whether cultured in 2D or 3D. Interestingly, this suggests that HMFs are more affected by culture conditions than DCIS cells. In addition, blank hydrogel controls (mixture of Matrigel and collagen) show a significant amount of IL6, IL8, TGFβ1, and VEGF without cells.

These observations support our hypothesis that 3D in vitro culture of HMF activates secretion of soluble paracrine signaling molecules that influence the invasive transition of MCF-DCIS cells. We further explored the influence of hepatocyte growth factor (HGF) on DCIS progression to IDC because HGF is a well-known scattering factor, a major contributor for invasive growth of cancer cells[31-33]. Jedeszko et al., for example, showed that, using a conventional 3D in vitro model and an in vivo model, mammary fibroblasts engineered for amplified HGF-secretion increased the percentage of DCIS structures with invasive outgrowth and activated c-Met[31].

However, their work did not compare the effect of fibroblasts cultured in 3D conditions and in 2D conditions on the scattering effect of DCIS in 3D in vitro systems.

Fibroblast-derived HGF production is increased in 3D in vitro culture and is necessary for progression of MCF-DCIS cells from a non-invasive to invasive phenotype.

HGF is a multi-functional cytokine stimulating invasion, motility, morphogenesis, as well as metastasis and is known to act through its specific receptor, c-Met on cancer cells[34-39]. Further, over-expression of HGF has been detected in various invasive carcinomas, including breast carcinomas, and high expression of HGF has been identified as a predictor of recurrence and shortened survival in breast cancer patients[32].

In our co-culture system, HMFs were the main source of HGF. We measured HGF mRNA expression in MCF-DCIS cells in both 2D and 3D conditions and found that it was not detectable under any conditions (Supplementary Fig. 2). Further, blank matrix did not release significant amounts of HGF (Supplementary Fig. 3). Thus, we concluded that the main source of HGF originates from the HMF cells. Further, we validated increased HGF production by HMF cultured in 3D using ELISA assays to analyze HMF cells cultured in various seeding densities in 2D, various matrix densities in 3D, and for different time points. HMFs in 3D conditions consistently produced more HGF than in 2D conditions (Supplementary Fig. 4). We also found that the production

of HGF was constant over the culture period, as the concentration of HGF at 48 hours was roughly double that of 24 hours (data not shown).

Next, we examined the effect of HGF on MCF-DCIS transition by inhibiting HGF activity with an HGF neutralizing antibody. 0.5 μg/ml of HGF neutralizing antibody was added to the conditioned media collected from 3D HMF cultures and a transwell invasion assay was performed. The addition of neutralizing antibody to the 3D conditioned media reduced the number of invaded cells to the level of the negative control. (Fig. 3). The conditioned media that did not contain the HGF neutralizing antibody displayed significantly higher invasion. These results indicate that HGF is the main paracrine factor modulating the invasion of MCF-DCIS cells, and that removal of this factor rescues the non-invasive phenotype.

Microfluidic 3D co-culture platform recapitulates the 2D/3D fibroblast effect observed in macroscale, allowing additional functional endpoints and enabling improved parametric control.

To further validate the difference between HMFs cultured in 2D and 3D we designed a microfluidic 3D co-culture platform that allows one to mix and match 2D and 3D co-cultures with short diffusion distances between the cell types. The system allowed us to co-culture MCF-DCIS cells in 3D with HMF cells in either 2D or 3D. Transwell systems have traditionally been used to perform combined 2D and 3D co-culture. However, these systems are limited in their ability to monitor the changes in both cell

types in a single experiment, require relatively large numbers of cells, and significant quantities of expensive matrix proteins (e.g. collagen, Matrigel). In addition, the surface areas and volume of the inserts in transwells (e.g., 0.3cm^2 and 0.2ml respectively in the 24-well format) are significantly smaller than the surface areas and volume of the bottom wells (e.g., 2.0cm^2 and 0.7ml respectively in the 24-well format), resulting in considerably different cell numbers and gel volumes between the bottom wells and the inserts.

Microfluidic 3D co-culture platforms have demonstrated unique functionality as well as an improved range of parameter control compared to traditional platforms. Accordingly, microfluidic platforms are emerging as a useful tools for examining complex interactions of tumor and stromal fibroblasts in various ECM conditions[27]. Microfluidic co-culture platforms provide additional capabilities over conventional transwell systems. The ability of microsystems to horizontally compartmentalize allows the monitoring of changes in cells and their associated ECM, and the isolation of paracrine signaling factors from juxtacrine signaling factors[27]. Second harmonic generation (SHG) is a powerful imaging technique that is becoming widely used to conduct label-free imaging of collagen and capture intrinsic characteristics of collagen networks[40-43]. In our study, we used SHG intensity to further define the invasive phenotype of the MCF-DCIS clusters (i.e., more invasive MCF-DCIS clusters alter ECM architecture at higher degree and exhibit higher SHG intensity values)[27]. Further, the microscale systems allow a reduction of at least 20 fold in cells and reagents use, saving resources, enabling an increase in the number of endpoints, and

enabling higher sensitivity to paracrine factors[44]. These systems also provide similar surface areas and sample volumes for two different cell types in distinct culture conditions. Finally, by leveraging physics at the microscale, accessible and reliable platforms can be developed that allow patterning of different cell types enabling novel 2D and 3D co-culture and tumor-stromal interaction studies[27].

We designed a simple compartmentalized microfluidic system composed of three connected cell-culture chambers: a central chamber for 3D culture of MCF-DCIS cells, and two outer chambers for 2D or 3D culture of HMFs (Fig. 4a). The central chamber was designed with a lowered height to facilitate pinning of fluid in that region[45], such that the fluid can be flowed into the central chamber from either side chamber and be passively retained when fluid is aspirated from either side chamber (Fig. 4a,b, supplementary Fig. 5, and supplementary movie 1). The surface areas of the center chamber and the two side chambers were designed to be roughly identical. The sample loading was completed in 3 simple steps (i.e., first injection, aspiration, and second injection), and did not require the use of fluids with matching viscosities as other laminar flow patterning based devices do[27]. The tubeless microfluidic method utilized for driving fluid flow is readily compatible with common pipetting methods, allowing increased throughput assays using a small number of cells[46-50]. We characterized the diffusion timescale and pattern of the device by conducing a fluorescent dye loading experiment using the fluorophore Texas Red bound to Dextran 70K MW (Fig. 4c and 4d, Supplementary Fig. 6).

The interaction of HGF and c-Met receptor was investigated by adding both HGF neutralizing antibody and c-Met inhibitor to examine whether blocking of either HGF or c-Met reduces the invasive transition of MCF-DCIS cells[37,51]. After 6 days of cultivation, samples were fixed and the morphology of MCF-DCIS clusters as well as SHG intensity were analyzed. The addition of HGF neutralizing antibody or c-Met inhibitor to the 3D HMF/3D MCF-DCIS co-culture significantly decreased the invasive transition of MCF-DCIS cells as quantified by the decreased AR of the clusters and decreased SHG intensity (Fig. 5a, supplementary Fig. 7a). The morphology change was negligible when the antibody and inhibitor were added to the 2D HMF/3D MCF-DCIS co-culture (Fig. 5b, supplementary Fig. 7b). This result is consistent with the previous findings that HMFs in 2D produce significantly lower amounts of HGF and correspondingly induce less activation of the c-Met pathway. In addition, we did not find a link between integrin β1 function and HGF production in this system in experiments utilizing integrin β1 blocking antibodies (Supplementary Fig. 8), suggesting that β1 integrin itself may not strongly contribute to the production of HGF. Based on the fact that there are 17 α subunits and 8 β subunits of integrins and these α and β subunits heterodimerize to produce 22 different complexes[52], it was not surprising to find that blocking one specific integrin did not disturb complex interactions between HMFs and various ECM compositions in the mixed matrix used in this work. Alternatively, integrins may play no role in regulating the secretion of HGF. Together, these findings show that stromal fibroblasts do participate in the invasive transition of tumor in vitro, but also that their culture conditions and microenvironmental cues are paramount in enabling that effect. Importantly, the

increased throughput, smaller volumes and lower reagent costs associated with the microscale culture platform will facilitate further “screening” investigations with integrins and other potential players to speed our understanding of the complex mechanisms involved in these phenomena.

Conclusions

The transition from DCIS to IDC is a critical stage in breast cancer progression, and improved understanding of the signaling mechanisms that regulate this transition can have clinical impact by identifying potential targets for alternative treatment options. The development and validation of models to study the invasive transition of breast cancer is central to advancing our understanding of the fundamental mechanisms involved. While the importance of 3D culture in in vitro systems and the influence of stromal fibroblasts in DCIS progression has been previously reported, this work provides strong evidence that the 3D environment itself affected stromal fibroblasts. The 3D culture of fibroblasts results in an increased secretion of signaling molecules compared to stromal fibroblasts cultured in 2D, subsequently enhancing the progression towards invasive phenotypes of the breast cancer cells. We have identified functional differences in HMF cultured in 2D vs 3D conditions. Specifically, the expression of HGF by HMF cultured in 3D is increased resulting in the transition of DCIS to IDC.

Further, we developed a microfluidic in vitro system to provide a more efficient and

physiologically relevant platform for the investigation of complex mechanisms involved in the cell-3D environment interaction. The microfluidic system enabled combined 2D/3D co-culture of MCF-DCIS and HMF cells using a simple pipette-driven loading process. Moreover, the side-by-side co-culture improved imaging capabilities by minimizing interference from the other cell type. The small volume required per endpoint and the compatibility with existing high-throughput infrastructure enables the use of various neutralizing antibodies and small molecule inhibitors with minimal cost and labor enabling screening approaches in 3D culture.

Materials and Methods

Cell culture

Human mammary fibroblast (HMF; originally termed RMF/EG) cells were provided by Dr. Kuperwasser[53] and were cultured in DMEM with high glucose and L-glutamine (Invitrogen, 11965-092, Grand Island, NY) supplemented with 10% calf serum (Invitrogen, 26010074, Grand Island, NY), and penicillin/streptomycin. MCF10-DCIS.com cells[54] were purchased from Asterand (Detroit, MI), and were cultured in DMEM-F12 with L-glutamine (Invitrogen, 11965-092, Grand Island, NY) supplemented with 5% horse serum (Invitrogen, 11320-033, Grand Island, NY), and penicillin/streptomycin. All cultures were maintained at 37 °C in a humidified atmosphere containing 5% CO2.

Cell line authentication

MCF10DCIS.com cells were authenticated by using “Cell Check” service provided by RADIL(http://www.radil.missouri.edu) on the date of September 26, 2011. The sample was confirmed to be of human origin and no mammalian inter-species contamination was detected. The alleles for 9 different markers were determined and the results were compared to the alleles reported for a previously submitted sample from Asterand. The genetic profile for the our sample was identical to the genetic profile of the Asterand sample reported previously.

Microchannel design, fabrication, and operation

The microfluidic devices were fabricated using multilayered SU-8 molds and PDMS-based soft-lithography. In brief, three layers of SU8-100 (Microchem Corp), of thicknesses 100 μm, 150 μm, and 500 μm, were spun on a 150 mm diameter silicon wafer and patterned according to the manufacturer's guidelines. UV lithography was performed using an Omnicure 1000 light source (EXFO) using masks printed on transparency (ImageSetter, Madison, USA). Subsequently, the wafer was developed using SU-8 developer (PGMEA, Sigma) and cleaned in acetone and IPA. Polydimethylsiloxane (Sylgard 184, Dow Corning) was mixed in a 1:10 cross-linker to base ratio, degassed for 30 min, and poured over the clean wafer on a hot plate. The molding process was performed by layering a transparency film, a layer of silicone foam, a 75 mm by 100 mm slab of glass, and a 5 kg weight on top of the wafer and PDMS, and baking the stack at 80°C for 3 hours. The cured PDMS layers were peeled off of the wafer, sterilized in 70% ethanol, and attached to polystyrene cell culture dishes (TPP AG, Switzerland). For multiphoton and confocal laser scanning

microscopy, PDMS channels were attached to a glass bottom culture dish (P50G-0-30-F, MatTek corp, Ashland, MA) after treating both the PDMS layer and the petridish in a plasma chamber for 50 seconds at 100W.

The channels were placed on ice for the loading and a cell suspension containing MCF-DCIS cells and a mixed matrix was loaded into one of the input ports until the fluid filled the center circular chamber. The excess cells in the side channels were removed by applying a gentle vacuum to the loading port. The cells-in-gel suspension was polymerized in a cell-culture incubator for 10 min by manually flipping the channels upside down every 2 min to prevent cell settling. The two side chambers were loaded with either a cell suspension of HMF cells in media, in a mixed matrix, or with blank gel.

Sample preparation for in vitro 3D culture

Collagen was prepared initially at a concentration of 5.0 mg/ml by neutralizing an acidic collagen solution (Collagen I, High concentration, rat tail, 354249, BD Biosciences) with 100mM HEPES buffer in 2X PBS (pH 7.7). For the collagen I only matrix condition, cells and culture media were added to neutralized collagen I gel to achieve a final concentration of 1.6 mg/ml. For mixed gel conditions, neutralized collagen gel and Matrigel (Basement Membrane Matrix, Growth Factor Reduced (GFR), Phenol Red-free, 10 ml *LDEV-Free, 356231, BD Biosciences) were mixed in equal volumes, and the collagen I concentration (0.8 mg/ml and 2.0 mg/ml) was adjusted by cell suspension and culture media. For loading into microfluidic channels,

the neutralized sample was kept at 4 °C for at least 15 min to apply an additional time for nucleation before channel loading[55].

Conditioned media collection

HMFs cultured in 2D proliferate faster than HMFs cultured in 3D, and, accordingly, we prepared lower cell densities for 2D samples ($3x10^4$ cells/48-well and $6x10^4$ cells/48-well) than the density of 3D samples ($1.2x10^5$ cells/48-well) in order to obtain similar final cell densities in the 2D and 3D samples after 48 hours. After cells were completely adhered to culture plates (for 2D samples) and to ECM (for 3D samples), serum-free media were added on top of samples. After 24 and 48 hours, conditioned media were collected and were centrifuged at 4000rpm for 5 min to pellet any floating cells and debris.

Invasion assay

The invasiveness of MCF-DCIS cells was assayed by using transwell invasion chambers (Matrigel Invasion Chambers in two 24-well plates, 8.0 μm, 354480, BD Biosciences). We resuspended MCF-DCIS cells in serum-free DMEM/F12 ($5x10^4$cells/ml), and seeded in the upper compartment of the chamber (0.2ml per chamber). The lower compartment was filled with 0.75ml of DMEM/F12 supplemented with different conditioned media collected from 2D and 3D cultures of HMF as a chemoattractant. After incubation at 37°C in a humid atmosphere for 36 hours, filters were rinsed with PBS. Remaining cells on the upper surface were wiped away with a wet cotton swab, and those on the lower surface were fixed with 4% paraformaldehyde, and stained

with Hoechst (Hoechst 33342, H3570, Molecular Probes). The number of invaded cells per microscopic view was counted and averaged.

Proliferation assays

For proliferation assays, 2D and 3D samples were fixed at each time point (0, 24 hours, and 48 hours) and nuclei stained with ToPro3. Cells were washed with 1xPBS then fixed with 4% paraformaldehyde for 30 min, and permeablized with 0.1% Triton X-100 in 1xPBS for 30 min at room temperature. ToPro3 was diluted 1:500 in PBS and incubated for 4 hours at room temperature, then washed three times with 1xPBS. The number of cells were estimated by scanning samples on an infrared (IR) laser scanner (Odyssey Licor Biosciences) to quantify integrated infrared intensity of ToPro3. The IR signal was calibrated by quantifying intensity values from different cell densities for 2D and 3D samples prior to perform proliferation assay (Supplementary Fig. 1).

Immunofluorescent staining

The samples were fixed in 4% paraformaldehyde in 1xPBS for 30 min at room temperature and, after 3 washes with 1xPBS, the cells were permeablized with 0.1% Triton X-100 in 1xPBS for 30 min at room temperature. For filamentous actin staining, phalloidin solution (1:50, Alexa Fluor 594 phalloidin, Invitrogen) was added, incubated at 4 °C for overnight, and washed 3 times with PBS.

Imaging and analysis

Brightfield images were acquired on an inverted microscope (Eclipse Ti-U, Nikon)

using the NIS-Element imaging system (Diagnostic Instruments, Inc.). F-actin and collagen fibers were imaged by using multiphoton laser scanning microscopy (with second harmonic filter for collagen). All multiphoton laser scanning microscopy (MPLSM) and Second Harmonic Generation (SHG) imaging was done on an optical workstation that was constructed around a Nikon Eclipse TE300. A MaiTai Deepsee Ti:sapphire laser (Spectra Physics, Mountain View, CA) excitation source tuned to 890 nm was utilized to generate both multiphoton excitation and SHG. The beam was focused onto the sample with a Nikon (Mehlville, NY) 20X Super Fluor air-immersion lens (numerical aperture (NA) = 1.2). All SHG imaging was detected from the back-scattered SHG signal with a H7422 GaAsP photomultiplier detector (Hamamatsu, Bridgewater, NJ), and the presence of collagen was confirmed by filtering the emission signal with a 445 nm (narrow-band pass) filter (TFI Technologies, Greenfield, MA) to isolate the SHG signal. Acquisition was performed with WiscScan (http://www.loci.wisc.edu/software/wiscscan), a laser scanning software acquisition package developed at LOCI (Laboratory for Optical and Computational Instrumentation, University of Wisconsin, Madison, WI). The morphology analysis of MCF-DCIS clusters was done by using shape descriptor measurement of ImageJ software for aspect ratio (major axis over minor axis).

Measurement of diffusion in microfluidic channels

The diffusion profiles in the microfluidic device were visualized using the fluorophore Texas Red bound to Dextran 70K MW (Invitrogen, Cat# D-1830) to obtain a diffusion coefficient closer to those of typical light paracrine signaling proteins. In brief, the

devices were loaded with a mixed gel in the center chamber, followed by a either the same mixed gel on the outer channels or with liquid media using the protocol previously described. The fluorophore was added to the media at a concentration of 1 μM. Immediately following the addition of the fluorophore, the devices were placed on the IX81 microscope stage (Olympus) and fluorescent timelapse microscopy was performed every 30 min for 9 hours. Images were retrieved and the intensity profile extracted using the software ImageJ. The diffusion pattern was compared to a numerical simulation performed on COMSOL using the 3D diffusion modeling toolbox. A subset of the device, not including the inlet and outlet ports for simplicity purposes, was modeled in 3D. The maximum mesh size was set to 50 μm, the diffusion coefficient of the gel was set to 10^{-10} $\mu m^2/s$, that of the liquid to $2x10^{-10}$ $\mu m^2/s$, and the fluorophore concentration was set to 0 in areas devoid of compound and 1 in areas containing the compound. A transient solver was used with solution stored every 15 min for a total time of 9 hours. The concentration profile was evaluated on a horizontal plane 50 μm above the floor of the channel, and heat-map images were exported at the desired times.

mRNA Transcription Analysis

mRNA was isolated from 2D or 3D cultured cells in 24-well using Dynabeads® mRNA DIRECT™ kit (Invitrogen, Cat# 610.21). Then mRNA was reverse transcribed to cDNA using high capacity cDNA reverse transcription kits from Applied Biosystems (Cat# 4374966). Real-time PCR was performed on StepOne Real-Time PCR System (Applied Biosystem) using TaqMan qPCR master mix (Applied Biosystems) along

primer/probe sets from Applied Biosystems for the HGF (Hs00300159_m1), MMP14 (Hs01037009_g1), COX2 (Hs01573471_m1), CXCL12 (Hs00171022_m1), and GAPDH (Hs99999905_m1) used as a housekeeping gene to normalize the total number of molecules in each sample. All PCR products had a denaturing step of 95 °C for 15 s, an annealing/extension step at 60 °C for 1 min for a total of 40 cycles. Quantification of mRNA was calculated using relative standard method. Standards are composed of five 1:10 serial dilutions of the same gene.

Zymography of MMPs Activity

To determine gelatinolytic and caseinolytic activities in HMF conditioned media, zymography was performed using gelatin and casein zymogram gels (Invitrogen). The assay was conducted by following manufacturer's protocols. Conditioned media from 2D and 3D cultures of HMF cells were collected at 48 hours culture. After being clarified by centrifugation, samples were mixed with 2xSDS sample buffer (Invitrogen) and then subjected to electrophoresis separation at 100V for 90 min. The gels were soaked in Renature buffer for 30min at RT and equilibrated in Develop buffer for 30 min. Then gels were incubated with Develop buffer overnight at 37°C to allow proteinase digestion of its substrate. Gels were stained using GelCodeTM Blue stain reagent (PIERCE) for 2 hours and then destained by DI water. Proteolytic activities appeared as clear bands of lysis against a blue background of stained gelatin or casein. To verify that the detected gelatinolytic and caseinolytic activities were specifically derived from MMPs, the gels were treated in parallel experiments with developing buffer containing 20mM of EDTA.

Bead-based ELISA

Six different conditioned media from 2D and 3D cultures of HMFs, MCF-DCIS cells, and blank gels were collected after 48 hours of cultivation as described above. Eight magnetic beads coated with specific capture antibodies were selected from three magnetic bead panels. Two Milliplex®$_{MAP}$ kits were purchased from Millipore (Human Adipokine Magnetic Bead Panel 2 (HADK2MAG-61K), Human Cytokine Magnetic Bead Panel (HCYTOMAG-60K)). One Bio-Plex Pro™ kit was purchased from Bio-Rad (TGF-β Standard 3-Plex). The assays were conducted by following manufacturer's protocols. After sample preparation was completed, 96-well plates were introduced into MagPix® instrument (Luminex Corporation) and data collected with xPONENT software (Luminex Corporation).

HGF ELISA

Conditioned media from 2D and 3D cultures of HMF cells were collected and clarified as above. Human HGF ELISA kit (Invitrogen) was used to detect HGF in conditioned medium. Briefly, 50 µl standard dilutions of recombinant human HGF and experimental conditioned media were dispensed into a 96-well plate coated with anti-HGF. The plate was sealed, incubated at room temperature for 3 hours and washed four times with washing buffer. After addition of 100 µl of biotinylated anti-Hu HGF solution and incubation for 1 hour at RT followed by four washes, 100 µl of Streptavidin-HRP was added and incubated for 30 min at RT. After 4 washes, 100µl of stabilized chromogen was added to the wells and incubated for 30 minutes, followed by addition of 100 µl of

Stop solution. The absorbance of each well was read at 450 nm using a SpectraMax Plus Spectrophotometer.

Acknowledgements

K.E.S led the project and performed experiments. D.J.B and A.F oversaw the project. K.E.S, E.B and D.J.B wrote the manuscript. X.S performed mRNA transcription analysis, zymography, and ELISA. E.B designed the microfluidic system used in this project and performed diffusion measurement. C.P performed SHG imaging and subsequent analysis.

References

1. Erler JT, Weaver VM (2009) Three-dimensional context regulation of metastasis. Clin Exp Metastasis 26: 35–49. doi:10.1007/s10585-008-9209-8.

2. Cukierman E, Pankov R, Yamada KM (2002) Cell interactions with three-dimensional matrices. Current opinion in cell biology 14: 633–639.

3. Bissell MJ, Radisky D (2001) Putting tumours in context. Nat Rev Cancer 1: 46–54. doi:10.1038/35094059.

4. Griffith LG, Swartz MA (2006) Capturing complex 3D tissue physiology in vitro. Nature Reviews Molecular Cell Biology 7: 211–224. doi:10.1038/nrm1858.

5. Ghajar CM, Bissell MJ (2008) Extracellular matrix control of mammary gland morphogenesis and tumorigenesis: insights from imaging. Histochem Cell Biol 130: 1105–1118. doi:10.1007/s00418-008-0537-1.

6. Nelson CM, Vanduijn MM, Inman JL, Fletcher DA, Bissell MJ (2006) Tissue geometry determines sites of mammary branching morphogenesis in organotypic cultures. Science 314: 298–300. doi:10.1126/science.1131000.

7. Cukierman E, Pankov R, Stevens DR, Yamada KM (2001) Taking cell-matrix adhesions to the third dimension. Science 294: 1708–1712. doi:10.1126/science.1064829.

8. Morales J, Alpaugh ML (2009) Gain in cellular organization of inflammatory breast cancer: A 3D in vitro model that mimics the in vivo metastasis. Bmc Cancer 9: 462. doi:10.1186/1471-2407-9-462.

9. Blobel CP (2010) 3D trumps 2D when studying endothelial cells. Blood 115: 5128–5130. doi:10.1182/blood-2010-03-275271.

10. Fischbach C, Kong HJ, Hsiong SX, Evangelista MB, Yuen W, et al. (2009) Cancer cell angiogenic capability is regulated by 3D culture and integrin engagement. Proc Natl Acad Sci USA 106: 399–404. doi:10.1073/pnas.0808932106.

11. Green JA, Yamada KM (2007) Three-dimensional microenvironments modulate fibroblast signaling responses. Advanced Drug Delivery Reviews 59: 1293–1298. doi:10.1016/j.addr.2007.08.005.

12. Grinnell F (2003) Fibroblast biology in three-dimensional collagen matrices. Trends Cell Biol 13: 264–269. doi:10.1016/S0962-8924(03)00057-6.

13. Kojima Y, Acar A, Eaton EN, Mellody KT, Scheel C, et al. (2010) Autocrine TGF- and stromal cell-derived factor-1 (SDF-1) signaling drives the evolution of tumor-promoting mammary stromal myofibroblasts. Proceedings of the National Academy of Sciences 107: 20009–20014. doi:10.1073/pnas.1013805107.

14. Orimo A, Gupta PB, Sgroi DC, Arenzana-Seisdedos F, Delaunay T, et al. (2005) Stromal fibroblasts present in invasive human breast carcinomas promote tumor growth and angiogenesis through elevated SDF-1/CXCL12 secretion. Cell 121: 335–348. doi:10.1016/j.cell.2005.02.034.

15. Ostman A, Augsten M (2009) Cancer-associated fibroblasts and tumor growth--bystanders turning into key players. Current Opinion in Genetics & Development 19: 67–73. doi:10.1016/j.gde.2009.01.003.

16. Hu M, Yao J, Carroll D, Weremowicz S, Chen H, et al. (2008) Regulation of in situ to invasive breast carcinoma transition. Cancer Cell 13: 394–406.

17. Hu M, Peluffo G, Chen H, Gelman R, Schnitt S, et al. (2009) Role of COX-2 in epithelial-stromal cell interactions and progression of ductal carcinoma in situ of the breast. Proc Natl Acad Sci USA 106: 3372–3377. doi:10.1073/pnas.0813306106.

18. Sharma M, Beck AH, Webster JA, Espinosa I, Montgomery K, et al. (2010) Analysis of stromal signatures in the tumor microenvironment of ductal

carcinoma in situ. Breast Cancer Res Tr 123: 397–404. doi:10.1007/s10549-009-0654-0.

19. Espina V, Mariani BD, Gallagher RI, Tran K, Banks S, et al. (2010) Malignant precursor cells pre-exist in human breast DCIS and require autophagy for survival. PLoS ONE 5: e10240. doi:10.1371/journal.pone.0010240.

20. Burstein HJ, Polyak K, Wong JS, Lester SC, Kaelin CM (2004) Ductal carcinoma in situ of the breast. N Engl J Med 350: 1430–1441. doi:10.1056/NEJMra031301.

21. Huang CP, Lu J, Seon H, Lee AP, Flanagan LA, et al. (2009) Engineering microscale cellular niches for three-dimensional multicellular co-cultures. Lab Chip 9: 1740–1748.

22. Chung S, Sudo R, Mack PJ, Wan C-R, Vickerman V, et al. (2009) Cell migration into scaffolds under co-culture conditions in a microfluidic platform. Lab Chip 9: 269–275. doi:10.1039/b807585a.

23. Du Y, Lo E, Ali S, Khademhosseini A (2008) Directed assembly of cell-laden microgels for fabrication of 3D tissue constructs. Proceedings of the National Academy of Sciences 105: 9522–9527. doi:10.1073/pnas.0801866105.

24. Wong A, Perez-Castillejos R, Love J, Whitesides G (2008) Partitioning microfluidic channels with hydrogel to construct tunable 3-D cellular microenvironments. Biomaterials 29: 1853–1861. doi:doi:10.1016/j.biomaterials.2007.12.044.

25. Chiu DT, Jeon NL, Huang S, Kane RS, Wargo CJ, et al. (2000) Patterned deposition of cells and proteins onto surfaces by using three-dimensional microfluidic systems. Proc Natl Acad Sci USA 97: 2408–2413. doi:10.1073/pnas.040562297.

26. Montanez-Sauri SI, Sung KE, Berthier E, Beebe DJ (2013) Enabling Screening in 3D Microenvironments: Probing Matrix and Stromal Effects on the Morphology and Proliferation of T47D Breast Carcinoma Cells. Integrative Biology. doi: 10.1039/c3ib20225a.

27. Sung KE, Yang N, Pehlke C, Keely PJ, Eliceiri KW, et al. (2011) Transition to invasion in breast cancer: a microfluidic in vitro model enables examination of spatial and temporal effects. Integrative Biology 3: 439–450. doi:10.1039/c0ib00063a.

28. Miller FR, Santner SJ, Tait L, Dawson PJ (2000) MCF10DCIS.com xenograft model of human comedo ductal carcinoma in situ. J Natl Cancer Inst 92: 1185–1186.

29. Dawson PJ, Wolman SR, Tait L, Heppner GH, Miller FR (1996) MCF10AT: a model for the evolution of cancer from proliferative breast disease. Am J Pathol 148: 313–319.

30. Su G, Blaine SA, Qiao D, Friedl A (2007) Shedding of Syndecan-1 by Stromal Fibroblasts Stimulates Human Breast Cancer Cell Proliferation via FGF2 Activation. J Biol Chem 282: 14906–14915. doi:10.1074/jbc.M611739200.

31. Jedeszko C, Victor BC, Podgorski I, Sloane BF (2009) Fibroblast hepatocyte growth factor promotes invasion of human mammary ductal carcinoma in situ. Cancer Res 69: 9148–9155. doi:10.1158/0008-5472.CAN-09-1043.

32. Elliott BE, Hung WL, Boag AH, Tuck AB (2002) The role of hepatocyte growth factor (scatter factor) in epithelial-mesenchymal transition and breast cancer. Can J Physiol Pharmacol 80: 91–102.

33. Nakamura T, Matsumoto K, Kiritoshi A, Tano Y, Nakamura T (1997) Induction of hepatocyte growth factor in fibroblasts by tumor-derived factors affects invasive growth of tumor cells: in vitro analysis of tumor-stromal interactions. Cancer Res 57: 3305–3313.

34. Grugan KD, Miller CG, Yao Y, Michaylira CZ, Ohashi S, et al. (2010) Fibroblast-secreted hepatocyte growth factor plays a functional role in esophageal squamous cell carcinoma invasion. Proc Natl Acad Sci USA 107: 11026–11031. doi:10.1073/pnas.0914295107.

35. Elenbaas B, Weinberg RA (2001) Heterotypic signaling between epithelial tumor cells and fibroblasts in carcinoma formation. Exp Cell Res 264: 169–184. doi: 10.1006/excr.2000.5133.

36. Haslam SZ, Woodward TL (2003) Host microenvironment in breast cancer development: epithelial-cell-stromal-cell interactions and steroid hormone action in normal and cancerous mammary gland. Breast Cancer Res 5: 208–215. doi: 10.1186/bcr615.

37. Cao B, Su Y, Oskarsson M, Zhao P, Kort EJ, et al. (2001) Neutralizing monoclonal antibodies to hepatocyte growth factor/scatter factor (HGF/SF) display antitumor activity in animal models. Proc Natl Acad Sci USA 98: 7443–7448. doi:10.1073/pnas.131200498.

38. Syed ZA, Yin W, Hughes K, Gill JN, Shi R, et al. (2011) HGF/c-met/Stat3 signaling during skin tumor cell invasion: indications for a positive feedback loop. Bmc Cancer 11: 180. doi:10.1186/1471-2407-11-180.

39. Rosário M, Birchmeier W (2003) How to make tubes: signaling by the Met receptor tyrosine kinase. Trends Cell Biol 13: 328–335.

40. Hompland T, Erikson A, Lindgren M, Lindmo T, de Lange Davies C (2008) Second-harmonic generation in collagen as a potential cancer diagnostic parameter. Journal of biomedical optics 13: 054050. doi:10.1117/1.2983664.

41. Han X, Burke RM, Zettel ML, Tang P, Brown EB (2008) Second harmonic properties of tumor collagen: determining the structural relationship between reactive stroma and healthy stroma. Optics Express 16: 1846–1859.

42. Zhuo S, Chen J, Xie S, Hong Z, Jiang X (2009) Extracting diagnostic stromal organization features based on intrinsic two-photon excited fluorescence and second-harmonic generation signals. Journal of biomedical optics 14: 020503. doi:10.1117/1.3088029.

43. Provenzano PP, Inman D, Eliceiri K, Knittel J, Yan L, et al. (2008) Collagen density promotes mammary tumor initiation and progression. BMC Med 6: 11.

44. Domenech M, Yu H, Warrick J, Badders NM, Meyvantsson I, et al. (2009) Cellular observations enabled by microculture: paracrine signaling and population demographics. Integrative Biology 1: 267–274. doi:10.1039/b823059e.

45. Atencia J, Beebe DJ (2005) Controlled microfluidic interfaces. Nature 437: 648–655. doi:10.1038/nature04163.

46. Walker G, Beebe D (2002) A passive pumping method for microfluidic devices. Lab Chip 2: 131–134.

47. Berthier E, Warrick J, Yu H, Beebe D (2008) Managing evaporation for more robust microscale assaysPart 2. Characterization of convection and diffusion for cell biology. Lab Chip 8: 860–864.

48. Montanez-Sauri SI, Sung KE, Puccinelli JP, Pehlke C, Beebe DJ (2011) Automation of three-dimensional cell culture in arrayed microfluidic devices. J Lab Autom 16: 171–185. doi:10.1016/j.jala.2011.02.003.

49. Puccinelli JP, Su X, Beebe DJ (2010) Automated high-throughput microchannel assays for cell biology: Operational optimization and characterization. JALA Charlottesv Va 15: 25–32. doi:10.1016/j.jala.2009.10.002.

50. Young EWK, Beebe DJ (2010) Fundamentals of microfluidic cell culture in controlled microenvironments. Chemical Society Reviews 39: 1036–1048. doi:10.1039/b909900j.

51. Gao C-F, Xie Q, Zhang Y-W, Su Y, Zhao P, et al. (2009) Therapeutic potential of

hepatocyte growth factor/scatter factor neutralizing antibodies: inhibition of tumor growth in both autocrine and paracrine hepatocyte growth factor/scatter factor:c-Met-driven models of leiomyosarcoma. Mol Cancer Ther 8: 2803–2810. doi:10.1158/1535-7163.MCT-09-0125.

52. Kumar CC (1998) Signaling by integrin receptors. Oncogene 17: 1365–1373. doi: 10.1038/sj.onc.1202172.

53. Kuperwasser C, Chavarria T, Wu M, Magrane G, Gray JW, et al. (2004) Reconstruction of functionally normal and malignant human breast tissues in mice. Proc Natl Acad Sci USA 101: 4966–4971. doi:10.1073/pnas.0401064101.

54. Tait LR, Pauley RJ, Santner SJ, Heppner GH, Heng HH, et al. (2007) Dynamic stromal-epithelial interactions during progression of MCF10DCIS.com xenografts. Int J Cancer 120: 2127–2134. doi:10.1002/ijc.22572.

55. Sung KE, Su G, Pehlke C, Trier SM, Eliceiri KW, et al. (2009) Control of 3-dimensional collagen matrix polymerization for reproducible human mammary fibroblast cell culture in microfluidic devices. Biomaterials 30: 4833–4841. doi: 10.1016/j.biomaterials.2009.05.043.

56. Hynes RO (2002) Integrins: bidirectional, allosteric signaling machines. Cell 110: 673–687.

Figure Legends

Fig. 1. 3D in vitro culture of HMF induce an increased transition of MCF-DCIS cells. (a) Conceptual illustration of the difference of HMF behaviors in 2D and 3D. Conditioned media collected from 3D culture of HMF (3D CM) stimulate invasive transition more than conditioned media collected from 2D culture of HMF (2D CM), and stimulate more invasive transition of MCF-DCIS cells in 3D. Outlines of MCF-DCIS clusters cultured in 3D mixed matrix with 3D CM and 2D CM. The clusters cultured with 3D CM produced more elongated clusters with aspect ratio (AR) 1.57. Scale bar is 100 μm. (b) Bar graph showing average aspect ratio of MCF-DCIS clusters cultured with control (serum free media, mono), 2D HMF (co-cultured with HMFs in 2D), and 3D HMF (co-cultured with HMFs in 3D). ‡ represents p value of 0.048. (c) Bar graph showing data obtained from transwell invasion assays with conditioned media from 2D culture of HMF (2D HMF) and 3D culture of HMF (3D HMF). ‡ represents p value of 0.022.

Fig. 2. HMFs in 3D produce more signaling molecules. (a) Conceptual illustration showing HMFs in 3D produce more signaling molecules. (b) Bar graphs showing the mRNA expressions of HGF, MMP14, COX2, and CXCL12 in HMFs cultured in 2D and 3D conditions. (c) Zymography showing the presence of increased active MMP2 in the 3D conditioned media of HMFs. (d) Bead-based ELISA showing the ratio of protein concentrations in conditioned media collected from 3D and 2D cultures of HMFs and MCF-DCIS cells.

Fig. 3. Invasion of MCF-DCIS cells with HGF neutralizing antibody (anti HGF) using transwells. The HGF neutralizing antibody (0.5 μg/ml) is added to 3D CM and BK CM (conditioned media collected from blank mixed gels). ‡ represents p value of 0.034.

Fig. 4. Microchannels used for 2D and 3D combined co-cultures of HMF and MCF-DCIS cells. (a) 3D schematic and cross-section of the microchannels used for 2D and 3D combined co-culture of HMF and MCF-DCIS cells. (b) Illustrations of the loading process showing the simplicity of loading both in 2D and 3D conditions. (c) Visualization of the diffusion process in the microdevice using a numerical COMSOL simulation and a timelapse microscopy of AlexaFluor488-Dextran10kD dye. (d) Average fluorophore concentration in the inner chamber of the microdevice plotted through time.

Fig. 5. MCF-DCIS clusters co-cultured with 3D HMF and with 2D HMF. (a) MCF-DCIS clusters (red and outlines) co-cultured with 3D HMF and neutralizing HGF antibody at 0.5 μg/ml (3D HMF-HGF). SHG (yellow) shows changes in collagen architecture around MCF-DCIS cells. The addition of HGF neutralizing antibody significantly decreased the aspect ratio of MCF-DCIS cells and the mean intensity of SHG. ‡ represents p value less than 0.05. (b) MCF-DCIS clusters (red and outlines) co-cultured with 2D HMF and neutralizing HGF antibody at 0.5 μg/ml (2D HMF-HGF). Scale bar is 100 μm.

Figure1_LZW

Click here to download high resolution image

Fig. 1. 3D in vitro cultures of HMF induce an increased transition of MCF-DCIS cells.

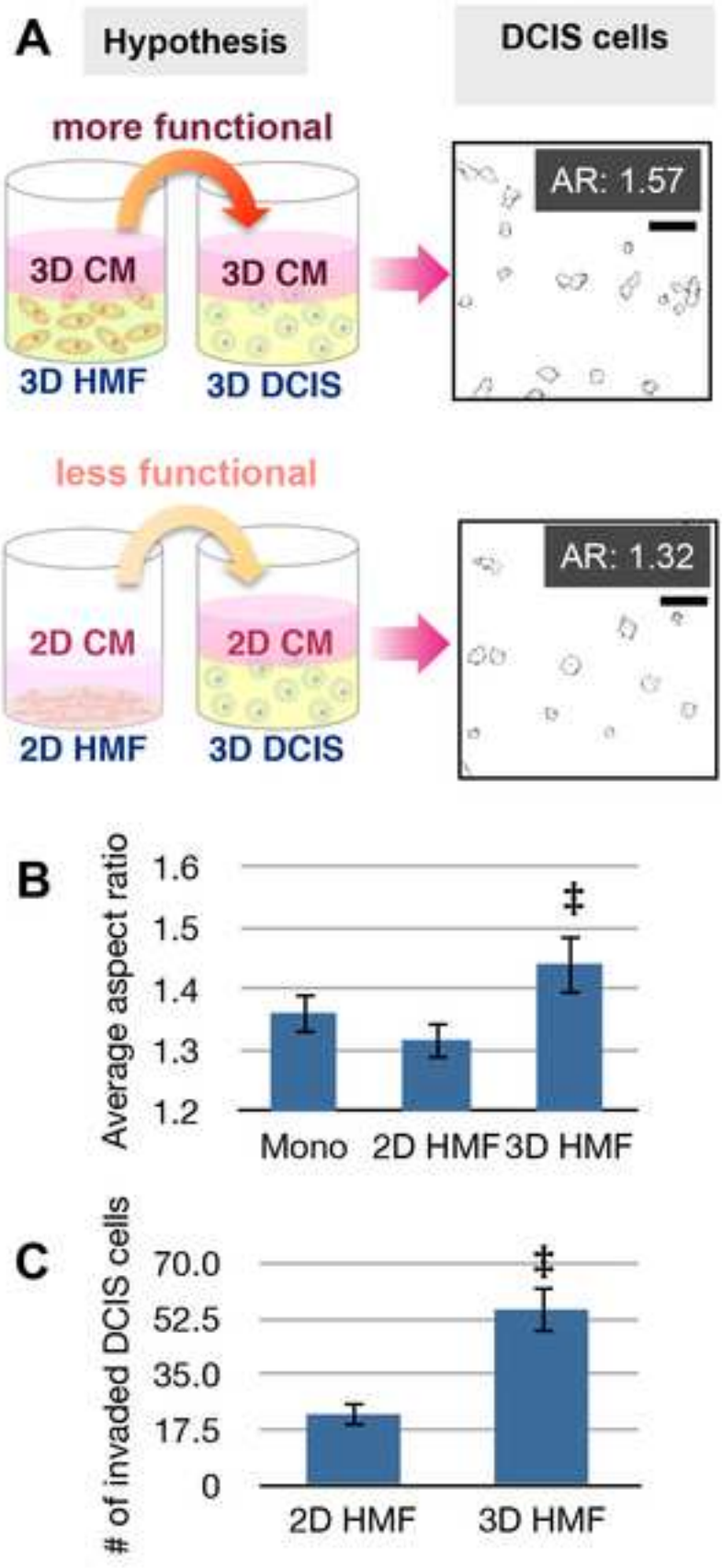

Figure2_LZW

Click here to download high resolution image

Fig. 2. HMFs in 3D produce more signaling molecules.

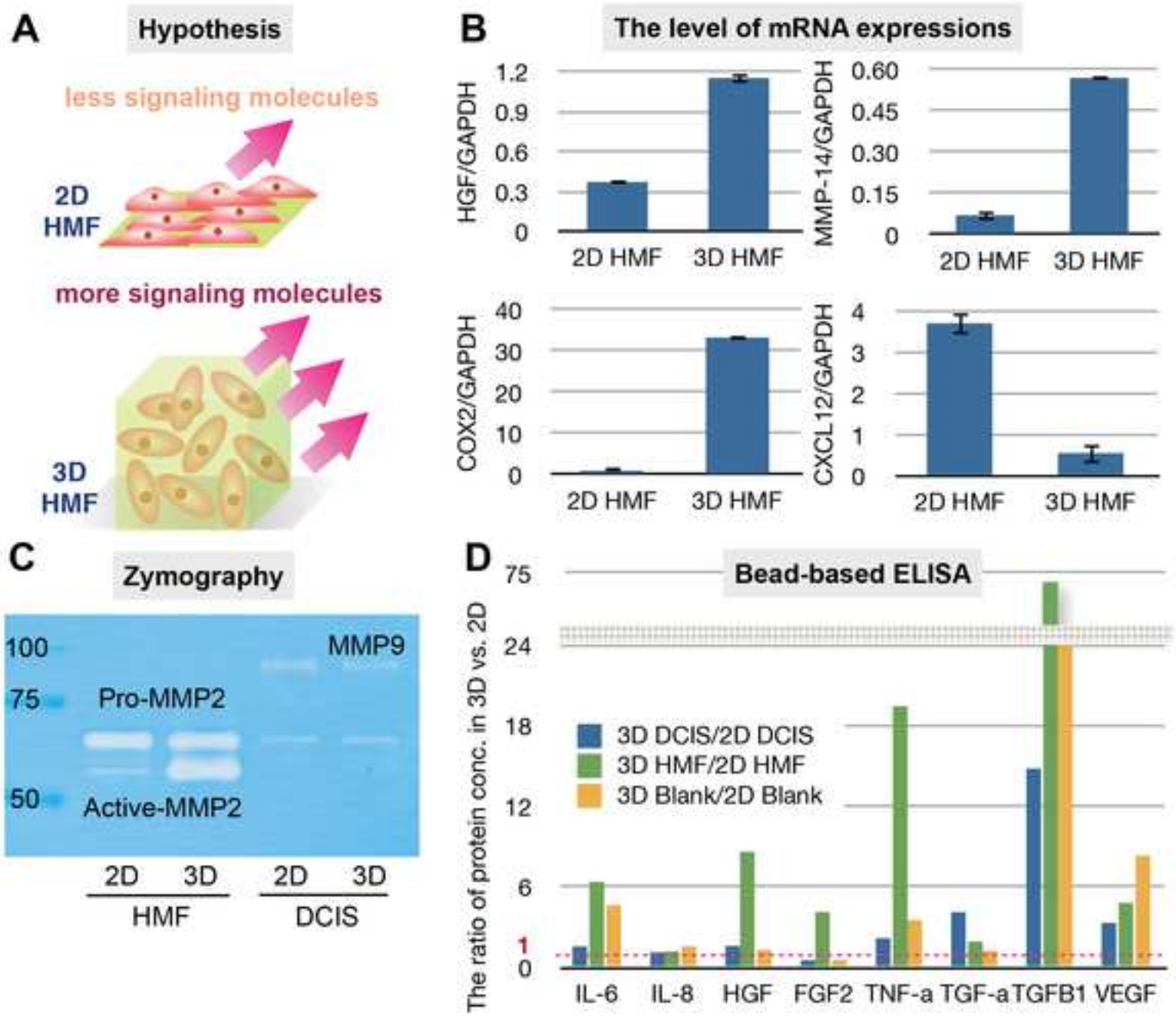

Figure3_LZW

Click here to download high resolution image

Fig. 3. Invasion of MCF-DCIS cells with HGF neutralizing antibody (anti HGF) using transwells.

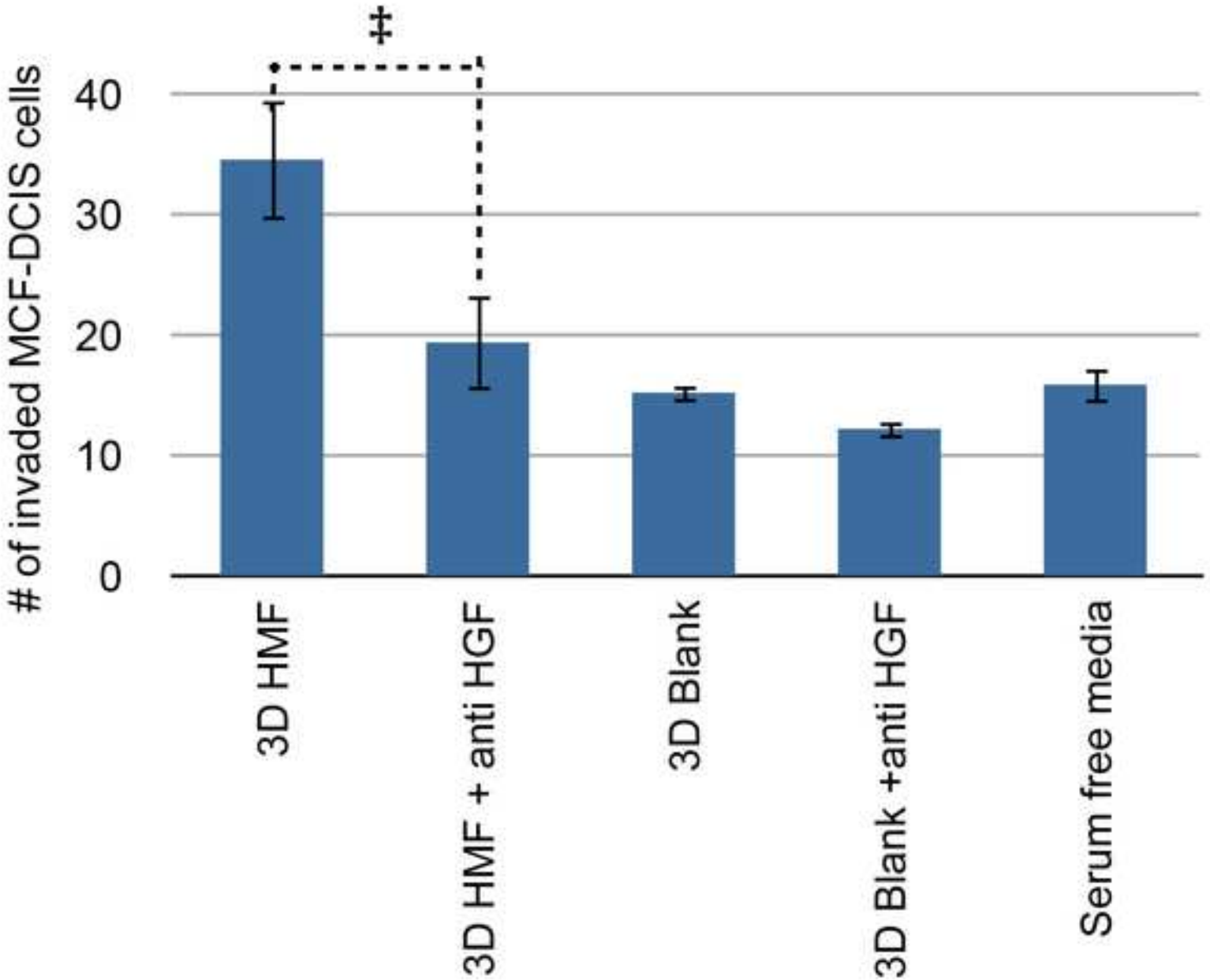

Figure4_LZW
Click here to download high resolution image

Fig. 4. Microchannels used for 2D and 3D combined co-cultures of HMF and MCF-DCIS cells.

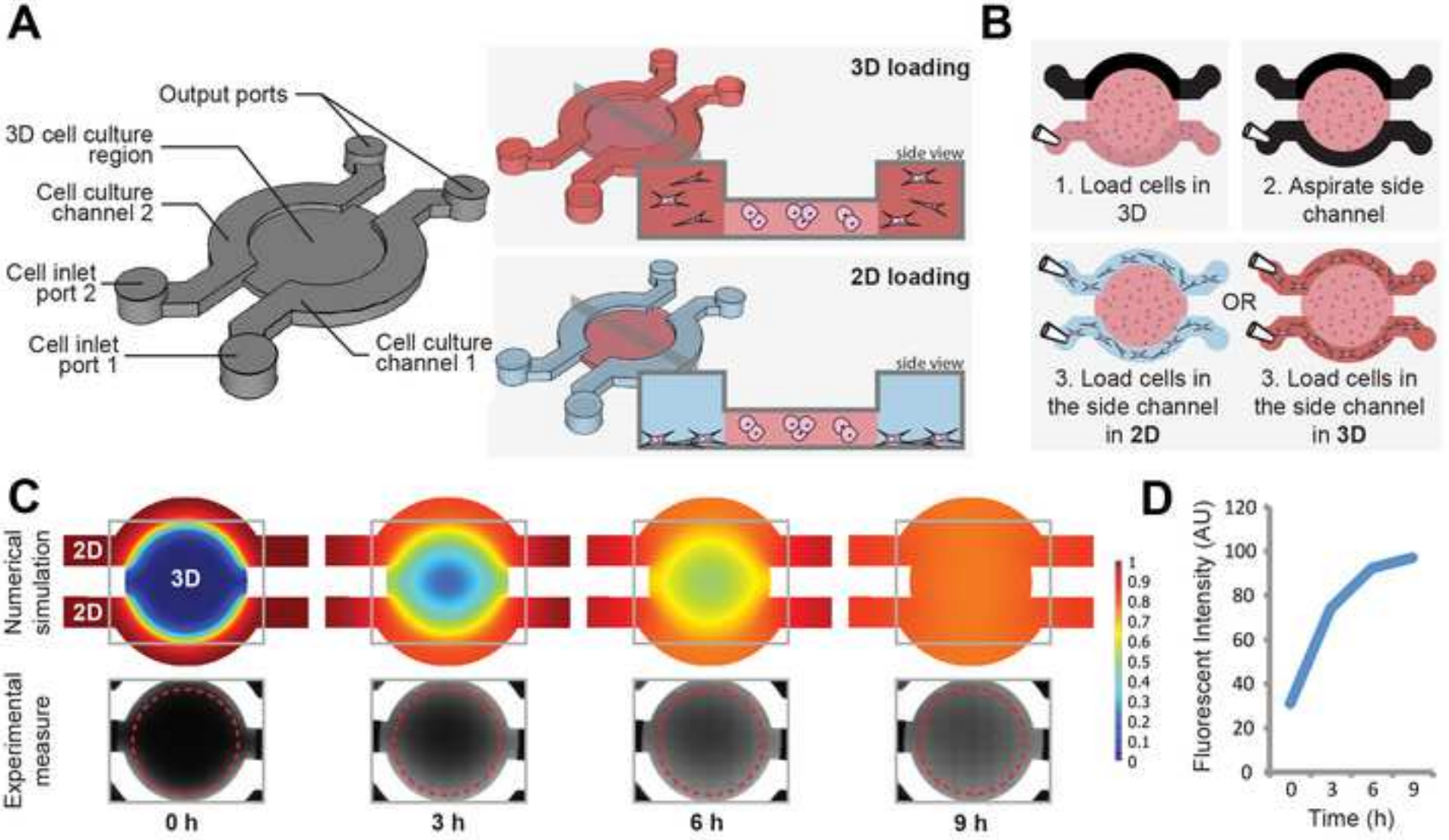

Figure5_LZW

Click here to download high resolution image

Fig. 5. MCF-DCIS clusters co-cultured with 3D HMF and with 2D HMF.

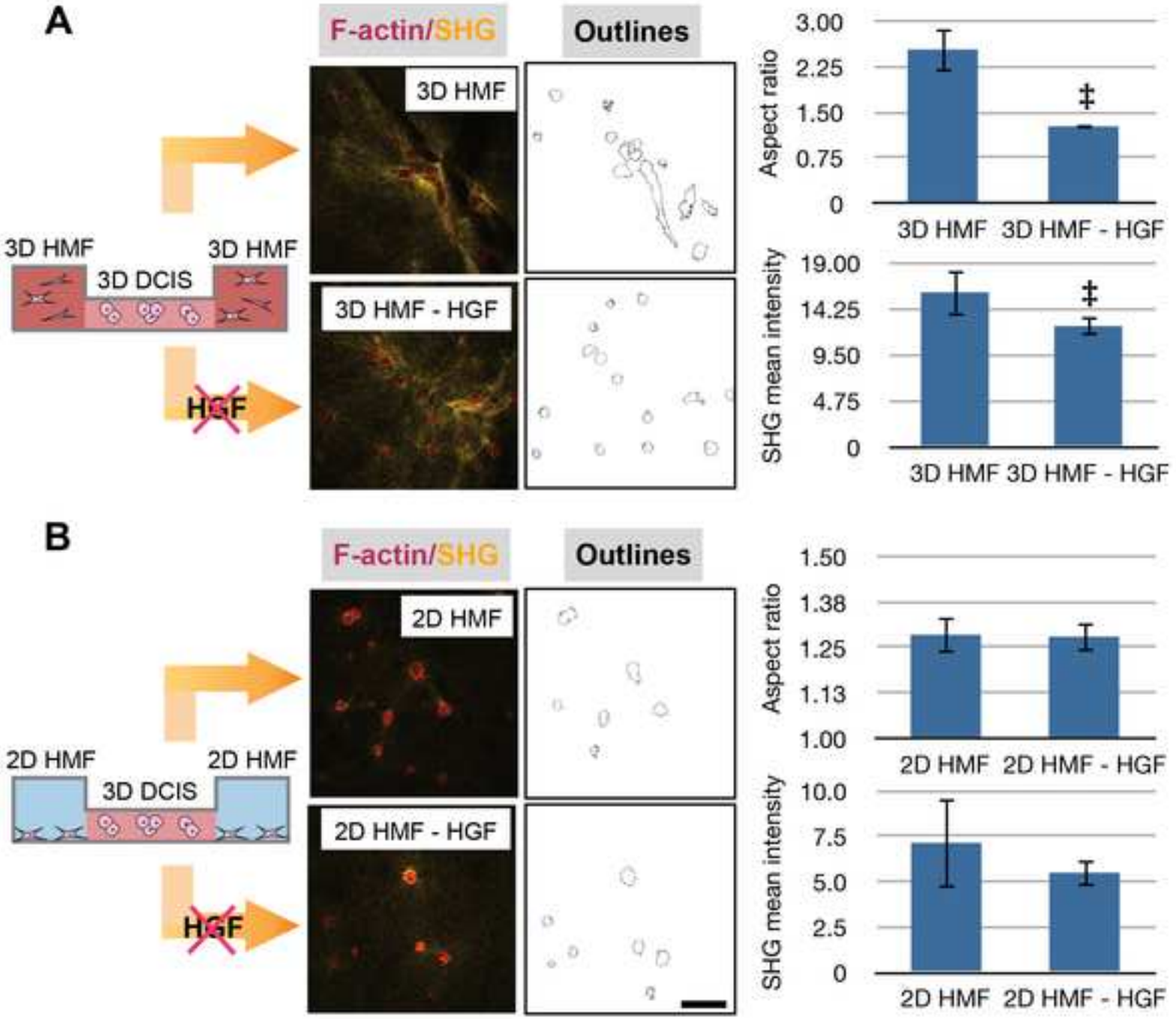

A micro scale 3D in vitro model of the breast cancer progression from DCIS to IDC: Deciphering the role of the stromal fibroblasts.

Kyung Eun Sung[1,4,5], Carolyn Pehlke[1,4,5], Erwin Berthier[3], Kevin W Eliceiri[1,4,5], Andreas Friedl[2,4,5], David J Beebe[1,4,5]

[1]Department of Biomedical Engineering, [2]Department of Pathology and Laboratory Medicine, [3]Department of Medical Microbiology and Immunology, [4]Paul P. Carbone Comprehensive Cancer Center, [5]Laboratory for Optical and Computational Instrumentation, University of Wisconsin, Madison, WI, USA

Breast cancer progression from ductal carcinoma in situ (DCIS) to invasive ductal carcinoma (IDC) is a critical step in breast cancer. This invasive transition of DCIS is defined by stromal invasion and is a life-threatening step accompanied by a dramatic drop in prognosis. In addition, the invasive transition of DCIS is largely driven by stromal alteration; thus it is critical to understand how DCIS alters the surrounding microenvironment, thus causing the cancer cells to become invasive. This study investigates the role of stromal fibroblasts in the vicinity of DCIS during the invasive transition using an innovative multidisciplinary approach that combines 3D cancer biology, microfluidics, and high-resolution imaging. We recently developed an efficient 3D microfluidic system that supports the transition from DCIS to IDC. The in vitro system employs microchannels with two inputs and one output enabling MCF10-DCIS.com cells (MCF-DCIS) and human mammary fibroblasts (HMF) to be loaded in two adjacent (side-by-side) compartments. This platform allows investigations of effects of spatial organization on the transition by independently analyzing their morphology and the modifications to the surrounding collagen architecture. Importantly, the compartmentalized platform enables monitoring of both MCF-DCIS and HMF independently including quantitative measures of the collagen architecture associated with each cell type. We observed that the HMF near MCF-DCIS became more protrusive versus HMF relatively far from MCF-DCIS. We have also begun to identify how the HMF become activated and protrusive when co-cultured with MCF-DCIS and to understand the biological function and impact of protrusive HMF during DCIS progression to IDC. We verified that the signaling based on Cathepsin D produced from MCF-DCIS and low-density lipoprotein receptor-related protein-1 (LRP1) from HMF is involved in regulation of the protrusive activity of HMF. Additionally, knocking down LRP1 in HMF inhibited the invasive transition of MCF-DCIS. This study demonstrates one possible route through which MCF-DCIS activate pre-existing fibroblasts and subsequently, leads to the modification of the ECM and the progression to IDC.